Contrib Mineral Petrol (2004) 147: 162–188
DOI 10.1007/s00410-003-0546-y

ORIGINAL PAPER

Eric H. Haskins · Michael O. Garcia

Scientific drilling reveals geochemical heterogeneity within the Ko'olau shield, Hawai'i

Received: 5 May 2003 / Accepted: 30 October 2003 / Published online: 7 February 2004

Abstract The Ko'olau Scientific Drilling Project (KSDP) was initiated to determine if the distinctive geochemistry of Ko'olau lavas is a near-surface feature. This project successfully deepened a recent, ~351 m deep, tri-cone rotary-drilled water well by coring another ~328 m. Three Ar–Ar plateau ages of 2.8 to 2.9 Ma from the drill core section of 103 flows confirm stratigraphic interpretations that core drilling recovered the deepest and oldest subaerially erupted lavas yet sampled from this volcano. The petrography and geochemistry of the core, and cuttings from this and another new Ko'olau water well (~433 m deep) were determined. These analyses revealed that the geochemically distinct lavas of Ko'olau form a veneer only 175–250 m thick at the drill sites, covering flows with more typical Hawaiian tholeiite compositions. The compositional change occurred near the end of shield volcanism and is not abrupt. Thus, it is probably not related to a catastrophic event such as the collapse of the northeast flank of this volcano. The distinct geochemistry of surface Ko'olau lavas cannot be explained by melting pyroxenitic or combined pyroxenitic and peridotitic sources. Additional recycled oceanic crustal components, such as plagioclase-rich cumulates and sediment, were probably involved. As the Ko'olau volcano drifted off the Hawaiian hotspot and the overall degree of melting decreased, the proportion of melts from recycled oceanic crustal material increased relative to those from mantle peridotite.

Electronic Supplementary Material Supplementary material is available for this article if you access the article at http://dx.doi.org/10.1007/s00410-003-0546-y. A link in the frame on the left on that page takes you directly to the supplementary material.

Editorial responsibility: T.L. Grove

E. H. Haskins · M. O. Garcia (✉)
Department of Geology and Geophysics, University of Hawai'i, 1680 East-West Road, Honolulu, Hawai'i 96822, USA
E-mail: garcia@soest.hawaii.edu
Tel.: +1-808-9566641
Fax: +1-808-9565512

Introduction

Among Hawaiian shield volcanoes, Ko'olau subaerial lavas are distinct in their major element, trace element, and isotopic compositions (e.g., Hauri et al. 1996). One remarkable feature of these lavas is their relatively high SiO_2, which has been interpreted to be the result of either a source component containing recycled oceanic crust (e.g., Hauri et al. 1996, Lassiter and Hauri 1998; Blichert-Toft et al. 1999) and/or lower pressure melting (Frey et al. 1994; Putirka 1999). The stratigraphic continuity of these geochemically distinct Ko'olau lavas has been questioned in several recent studies. Work on flows exposed deep within a new highway tunnel (Jackson et al. 1999) and from the submarine flanks of the volcano (Tanaka et al. 2002; Shinozaki et al. 2002) have unexpectedly revealed compositions resembling lavas from the Kīlauea and Mauna Loa volcanoes, respectively. These findings suggest that the geochemically distinct lavas of Ko'olau form only a thin veneer over more typical Hawaiian tholeiites. If this hypothesis is correct, then obtaining an ordered sequence of lava samples beneath the exposed surface of the volcano could reveal a dramatic geochemical transformation within the main growth stage of this volcano and help assess the relative role of source versus process in creating these chemical differences. Such a transition within Ko'olau would be in striking contrast to the relatively uniform major element compositions of Kīlauea and Mauna Loa shield-stage lavas over time (Rhodes 1996; Quane et al. 2000) and the predicted behavior of a volcano over the Hawaiian mantle plume (e.g., Hauri and Kurz 1997). The volume of this unusual component can be determined by evaluating geochemical changes with depth for Ko'olau lavas.

Core drilling is the best approach for obtaining a stratigraphic sequence from the interior of the volcano. We anticipated that drilling on the leeward side of the Ko'olau range would reduce the effects of surface weathering (e.g., Frey et al. 1994) and produce less altered samples for geochemical analyses and dating. Also, core

drilling would provide an excellent stratigraphic section for paleomagnetic studies, which might better constrain the age of Ko'olau volcanism. This paper documents the stratigraphy, geochronology, petrography, and major and trace element geochemistry of lavas from the 679-m deep Ko'olau Scientific Drilling Project (KSDP) hole and the ~433 m deep Wa'ahila Ridge water observation well. A separate study (Herrero-Bervera et al., unpublished data) examines the paleomagnetic features of the core. Here we show that the distinctive geochemical characteristics of Ko'olau shield lavas is characteristic of only its final stage of growth. Parent magmas for these lavas have not been created by experimental studies of melting peridotite or peridotite–basalt mixtures; additional oceanic crust components are needed.

Geologic setting

The extinct Ko'olau volcano makes up the eastern part of the island of O'ahu in the Hawaiian archipelago. Its subaerial lavas, dated by K–Ar methods at 1.8–2.7 Ma (McDougall 1964; Doell and Dalrymple 1973; all K–Ar ages converted to constants of Steiger and Jaeger 1977), overlie those of the adjacent Wai'anae volcano (K–Ar ages of 2.9–3.9 Ma; Doell and Dalrymple 1973; Presley et al. 1997, Guillou et al. 2000). The subaerially exposed remains of the Ko'olau volcano preserve its basic, elongate shield form, consisting of a NW-trending dike complex and two shorter rifts extending ESE and SW from the now deeply eroded caldera (Fig. 1a). The catastrophic Nu'uanu landslide is thought to have carried away most of the eastern portion ($2.9–3.8 \times 10^3$ km^3) of the Ko'olau volcano, approximately 40% of its volume, littering the seafloor with giant blocks up to 40 km long for distances up to 150 km (Moore et al. 1989; Satake et al. 2002). The timing of this event is not well known, but is likely to have occurred near the end of the shield-building stage based on the partial filling of the amphitheater left by the landslide. The final stage of Ko'olau volcanism apparently did not produce an alkalic cap, which is found on most Hawaiian shield volcanoes. After ~1 Ma of erosion and at least 1 km of subsidence, rejuvenation-stage eruptions began on the Ko'olau shield (Clague and Dalrymple 1987; Moore 1987). Rejuvenated activity produced ~40 monogenetic eruptions of moderately to strongly silica-undersaturated magma from 0.9 to 0.03 Ma (Gramlich et al. 1971; Lanphere and Dalrymple 1980). This eruptive material is commonly referred to as the Honolulu Volcanics. One such eruption, which formed the Salt Lake tuff cone, blasted out bombs of shield-stage Ko'olau tholeiite. Two of these Ko'olau samples are discussed below.

The KSDP drill site (Fig. 1a) is located on the western margin of lower Kalihi Valley. The valley was incised into the Ko'olau shield and later partially filled by nepheline melilitite lavas from two rejuvenated-stage eruptions Wentworth 1951). The older eruption produced the Kalihi flow from a vent near the head of the valley (Fig. 1a, location 1). K–Ar dates of the Kalihi flow are 470 ± 12 ka (Gramlich et al. 1971) and 580 ± 25 ka (Lanphere and Dalrymple 1980). Later, the Kamanaiki rejuvenated flows erupted from one or more vents on the east side of Kalihi Valley (Fig. 1a, location 2). These flows are thought to contain slightly more melilite and less pyroxene and nepheline than the Kalihi flow (Winchell 1947). The Kamanaiki eruption has not been dated, but is likely to be 50–100 ka younger based on stratigraphic relationships with dated units (Winchell 1947).

The relative position of the KSDP drill site below the volcano's paleoshield surface can be estimated using the slopes of Ko'olau's leeward ridges, adjusted for erosion. Wentworth and Winchell (1947) used these ridges to make an estimate of the maximum extent of shield growth. The KSDP drill site is located about 150 m below the pre-erosional surface. Drilling of another water observation well on one of these ridges (Wa'ahila, location 4, Fig. 1a) intersected rock no more than 10–50 m below the shield's pre-erosional surface.

The stratigraphic height of the drill core section site with respect to previous Ko'olau stratigraphic studies was estimated based on our fieldwork in Kalihi and that of Jackson et al. (1999) at the H3 tunnels (Fig. 1a). Both studies found an average regional lava flow dip of 4° to the south (away from the caldera), although dips varied in the range 0.5–8° in lower Kalihi Valley due to irregular underlying surface flow topography. A cross section of the Ko'olau volcano through Kalihi Valley was constructed between these field sites using the 4° regional dip (Fig. 1b). Based on this cross section, it was anticipated that the rotary-drilling phase of the KSDP would sample a similar but less altered stratigraphic interval as the H3 tunnel section. Core drilling was expected to extend at least 300 m beyond the stratigraphic equivalent of the deepest Ko'olau subaerial exposure. The flows cored would, therefore, sample deeper portions of the volcano than any previous study and allow us to evaluate the suggestion of Jackson et al. (1999) that the geochemically distinct lavas of the Ko'olau volcano may form a relatively thin surface feature covering lava with more typical Hawaiian shield compositions. The Wa'ahila Ridge well provides a second section through the potential transition zone, sampling the same interval as the KSDP rotary-drilled section and the uppermost 25% of the cored section.

Methods

Rotary and core drilling

Rotary drilling of the Honolulu Board of Water Supply (HBWS) Kalihi groundwater observation well in 1999 reached a depth of 303.7 m b.s.l. (~351-m total depth; Fig. 2). Drillers sampled rock cuttings every 2–3 m, although no cuttings were returned from the 90–173 m b.s.l. depth interval. We sieved cuttings every 5–10 m to obtain fragments > 2 mm. These chips were washed, dried, and then examined with a binocular

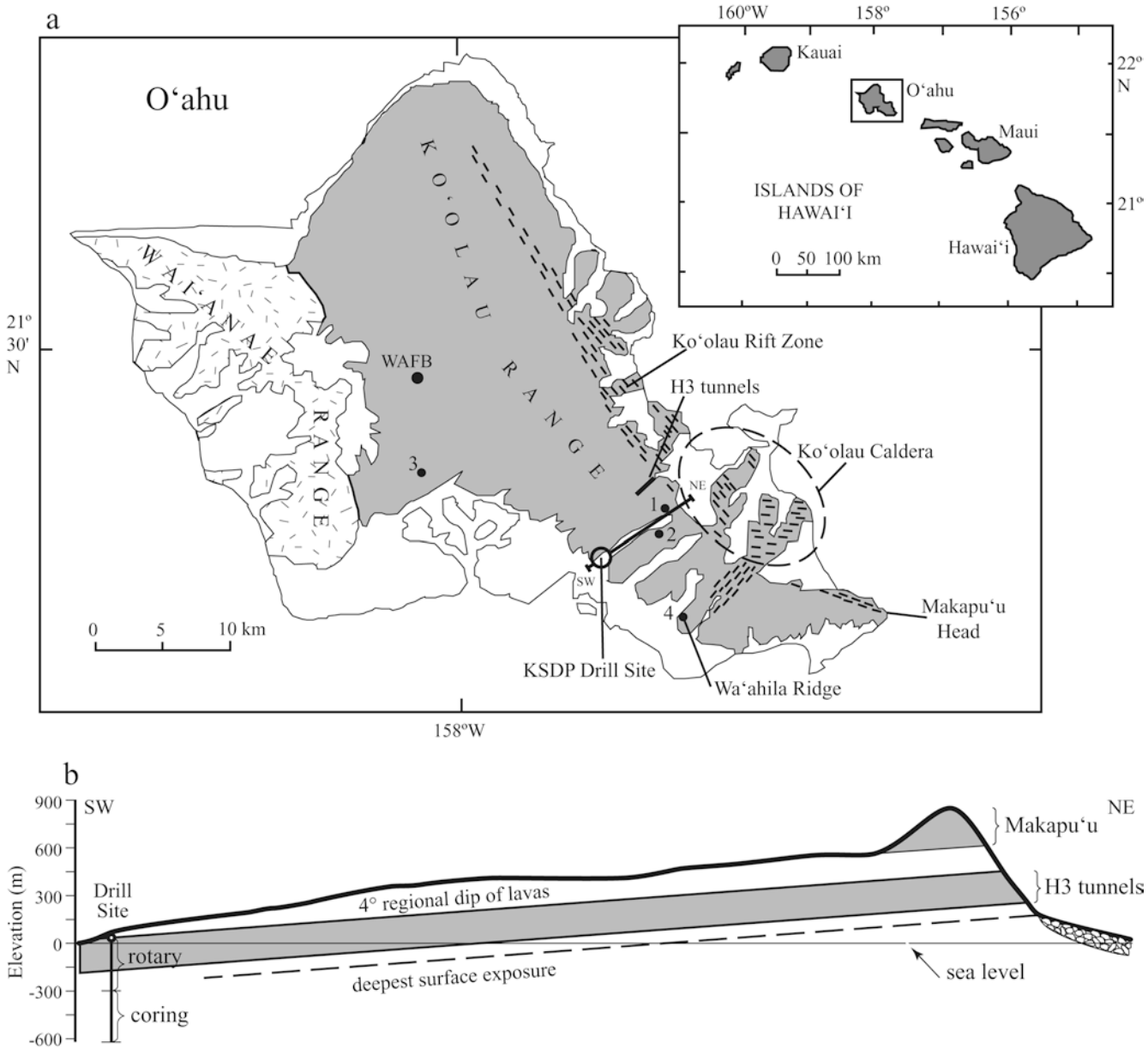

Fig. 1a, b Geology of the island of O'ahu. **a** Map showing the eroded remnants of Ko'olau (*shaded*) and Wai'anae (*hatched*) shield volcanoes (modified from Jackson et al. 1999). The rift zones and caldera of Ko'olau are shown by *dashed lines*, as well as previous study sites (Makapu'u Head, H3 tunnels, and the Wheeler Air Force Base, *WAFB*). The KSDP drill site is located in lower Kalihi Valley. Locations labeled *1* and *2* are for the Kalihi and Kamanaiki rejuvenation-stage vents, respectively (Wentworth 1951); locations *3* and *4* are the lava flow dip study sites of Multhaup (1990). The line SW–NE shows the location for a cross section (**b**) of the upper lavas of Ko'olau through Kalihi Valley. The 4° regional dip observed at the H3 tunnels (Jackson et al. 1999) and in outcrops near the KSDP site was used in the section. The relative stratigraphic positions of the previous studies are projected to the drill site. The deepest surface exposure from the Kaneohe Pali is also shown

microscope to select unaltered samples for thin section petrography and XRF major element analyses. A total of 28 intervals were selected for thin sections and, based on thin section examination, 17 samples were chosen for XRF. For comparison, cuttings from another HBWS well 8.5 km southeast of the KSDP on Wa'ahila Ridge (drilled to a total depth of ~433 m; location 4 on Fig. 1a) received the same sampling and examination procedures (23 thin sections and 12 XRF analyses). For comparison,

►

Fig. 2 Graphic logs for the rotary-drilled Wa'ahila Ridge and the rotary-drilled and cored sections of the KSDP holes. All elevations are relative to sea level; note scale change for cored section. Within the rotary sections, the large double-ended *arrows* are for zones where the rocks were deeply weathered (Wa'ahila) or not recovered (KSDP). The *square* and *circle* denote where rocks were taken for thin section and XRF analyses, respectively, in the rotary-drilled sections. *Stars* denote the locations of the three samples with successful Ar–Ar age determinations. *Dashed lines* mark a change in lithology; *solid vertical lines* indicate mixed flow types within the sampling interval. See Table 2 for flow-type determination critera. *T.D.* Total depth

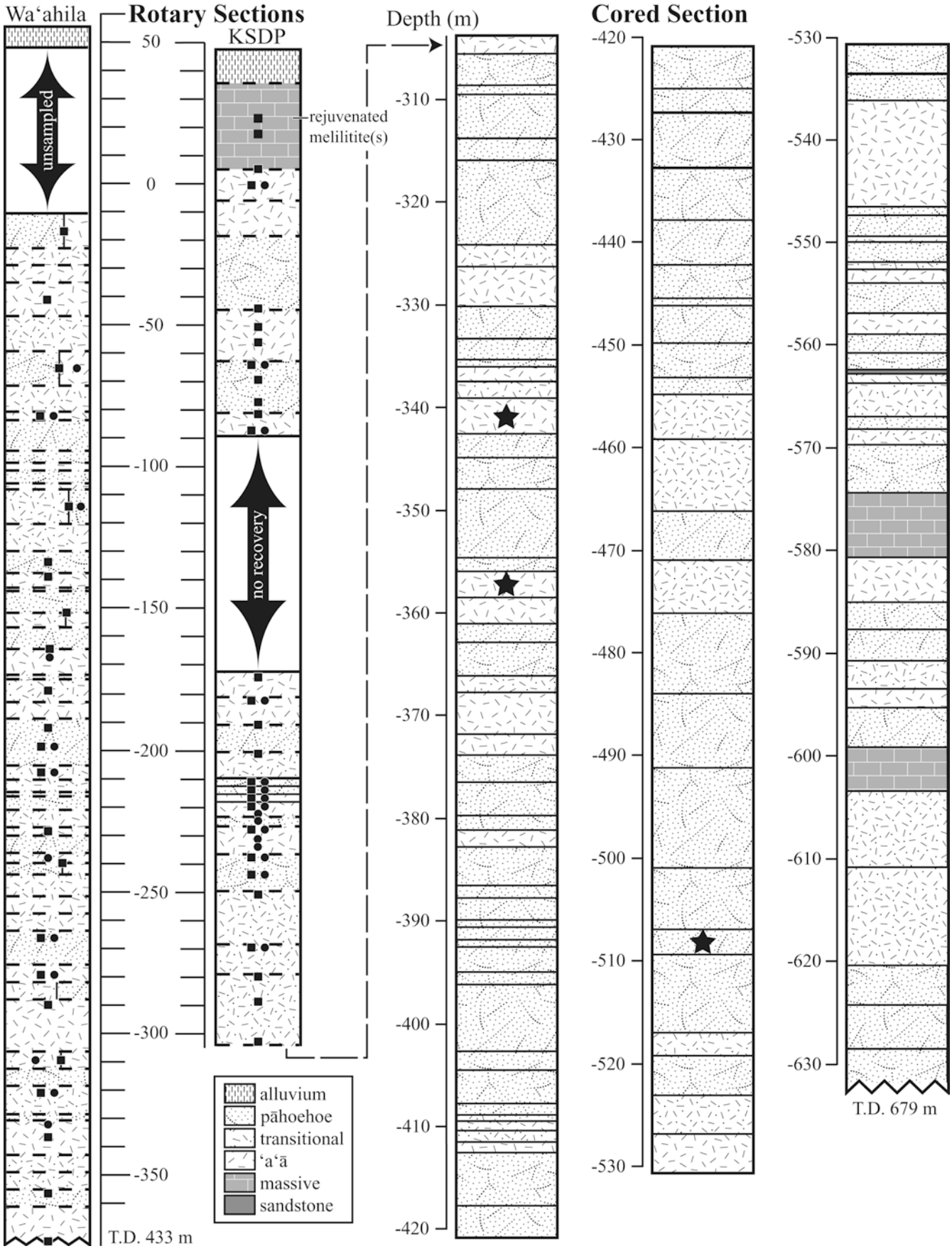
Wa‘ahila
Rotary Sections
KSDP
Depth (m)
Cored Section
unsampled
rejuvenated
melilitite(s)
no recovery
50
0
-50
-100
-150
-200
-250
-300
-350
T.D. 433 m
-310
-320
-330
-340
-350
-360
-370
-380
-390
-400
-410
-420
-420
-430
-440
-450
-460
-470
-480
-490
-500
-510
-520
-530
-530
-540
-550
-560
-570
-580
-590
-600
-610
-620
-630
T.D. 679 m
alluvium
pāhoehoe
transitional
‘a‘ā
massive
sandstone

we evaluated the geochemistry of core from the Wheeler Air Force Base (WAFB; Takeguchi and Takahashi, unpublished data; Fig. 1a), along with the results of our analyses. The WAFB section is 200 m thick with 29 flows of Ko'olau lavas. All 14 of the flows suitable for paleomagnetic analysis have reversed inclinations. Two of these units, KO19 (126 m deep) and KO25 (163 m deep), have unspiked K/Ar ages of 2.11 ± 0.04 and 2.10 ± 0.04 Ma, respectively (Laj et al. 2000), indicating that they were erupted just after the normal polarity Réunion event (2.14–2.15 Ma; Cande and Kent 1995).

Core drilling services for the KSDP were provided by DOSECC (Drilling, Observation, and Sampling of the Earth's Continental Crust), using their newly built GLAD800 rig. Drill rig specifications are given at the DOSECC website at http://www.dosecc.org/html/glad800.html. The coring utilized a 9.3-cm outer diameter diamond drill bit to produce 6.1-cm-diameter core that was fed into a ~3 m barrel. When this barrel was full or blocked, it was pulled to the surface by a wire line while the core bit and rods remained in the hole. Core handling and logging was conducted according to procedures developed during the Hawaii Scientific Drilling Project (HSDP; Seaman et al. 1999).

Petrologic logging

The KSDP penetrated ~679 m, reaching a final depth of 632 m b.s.l. The presence or absence of soil, baked material, or glassy surfaces was used along with petrography to define lithologic units. Each lava unit was point counted twice with a transparent sheet containing a 100-point overlay grid to determine the olivine, plagioclase, and vesicle abundances. Groundmass size, vesicularity, extent of alteration, fracturing, and other features such as autoliths, flow banding, ropy pāhoehoe surface textures, and volcanic glass were noted. Lithologic units were assigned flow types ('a'aā, paāhoehoe, transitional, or massive; Table 1) based on their characteristics. 'A'aā flows generally have elongate vesicles, cryptocrystalline matrix, and a massive interior between layers of clinker. Pāhoehoe flows have spherical vesicles, microcrystalline matrix, and commonly contain multiple lobes. Transitional flows have characteristics of both 'a'aā and paāhoehoe, while massive flows have few vesicles and no internal lobes or clinker layers.

Contact locations were annotated on box photographs, as were locations where point counts were taken, unit numbers, and other notable features. Detailed logging descriptions, box photographs, daily reports of drilling activities, and additional information about the KSDP can be found at http://www.icdp-online.de/sites/koolau/news/news.html.

Geochemical analyses

Whole-rock major and trace element abundances from the KSDP and Wa'ahila Ridge were determined by X-ray fluorescence (XRF) at the University of Massachusetts (UMass). This laboratory produced analyses of Ko'olau lavas from the Makapu'u and H3 study sites (Frey et al. 1994; Jackson et al. 1999), so these analyses can be compared with the new KSDP data without concern for interlaboratory bias.

Core samples were selected for geochemical analysis from the freshest portions of the least altered flows (88 of the 104 identified lithologic units). For comparison, a surface basalt sample (~50 m a.s.l.) was taken from a tunnel entrance in the ridge adjacent to the drill site. Dried samples were ignited overnight and powdered in an agate mortar before being weighed. Major element precision and accuracy for SiO_2, TiO_2, Al_2O_3, Fe_2O_3, MgO, CaO, and K_2O is typically better than 0.5% for Hawaiian tholeiitic basalts, except MnO, Na_2O, and P_2O_5, which are usually within 0.5–1% (1σ error; Rhodes 1996). Loss on ignition (LOI) was determined by heating approximately 5 g of sample in a Pt:Au (95:5) crucible at 1,020 °C for at least 10 h. Whole-rock trace element abundances were determined for each sample using the procedures of Norrish and Hutton (1969) and Chappell (1991). Trace element (V, Cr, Ni, Zn, Rb, Sr, Y, Zr, Nb, Ba, and Ce) precision and accuracy at 1? is typically within 0.5–2% (Rhodes 1996).

Chips from the rotary-drilled sections were selected where unaltered rock of a uniform rock type was present. The fewest possible number of fragments (1–8) were used to obtain the 300 mg of powder required for one major element analysis. Insufficient material was available for XRF trace element analyses, which require 10 g.

Volcanic glass major element abundances from KSDP flow and intraflow contacts were determined by electron microprobe analysis at the University of

Table 1 Summary of flow type, lithology, and flow thickness (m) for KSDP rock cores

Flow type	No. of flows	Picritic basalts[a]	Olivine basalts	Basalts	Total thickness	Mean thickness	Vol%
Pāhoehoe	67	7	17	43	211.9	3.2	64.7
Transitional	19	1	3	15	58.5	3.1	17.9
'A'ā	15	3	2	10	46.5	3.1	14.2
Massive	2	2	0	0	10.7	5.3	3.2
Total	103	13	22	68	327.6	3.2	100.0

[a]Picritic basalts, > 12% olivine; olivine basalts, 5–12% olivine; basalts, < 5% olivine

Table 2 Vesicle-free modal mineralogy for KSDP core lavas (volume %, based on 500-point counts)

Unit	Depth	Groundmass	Ol		Opx		Plag		Cpx		Opq	A.I.[a]
	(m)	(%, c, m)	Ph	Mph	Ph	Mph	Ph	Mph	Ph	Mph	Mph	(1–5)
1	–303.8	65.0	20.2	-	3.2	-	9.6	-	2.0	-	-	2
2	–308.3	56.2	26.6	-	4.6	-	7.0	3.2	1.6	0.8	-	2.5
3	–308.9	49.4	32.8	-	4.6	-	5.4	4.2	2.2	1.4	-	3
4	–312.3	85.2	7.8	-	-	-	-	5.4	-	1.2	0.4	2.5
5	–314.5	81.6	17.8	-	-	-	-	-	0.6	-	-	3
6	–316.8	79.4	20.0	-	-	-	-	0.4	-	-	0.2	2.5
7	–325.3	87.4	12.4	-	-	-	-	-	-	-	0.2	2.5
8	–329.0	86.4	10.8	-	-	-	0.2	2.2	-	0.4	-	1.5
9	–332.4	90.2,	5.6	-	2.4	0.8	0.2	0.6	-	-	0.2	2
10	–334.5	93.6	3.4	-	3.0	-	-	-	-	-	-	3
12	–336.2	92.4	2.0	-	4.6	-	-	1.0	-	-	-	2.5
13	–338.0	94.6	3.0	-	-	-	0.2	2.2	-	-	-	2.5
14	–342.0	90.8	5.2	-	-	-	0.2	2.8	0.2	0.8	-	2
15	–343.9	81.6	10.4	-	-	-	0.2	4.6	-	3.0	0.2	2.5
16	–345.5	91.0	2.0	-	-	-	-	3.8	1.0	1.8	0.4	2.5
17	–350.4	97.2	1.2	-	-	-	0.8	0.2	-	0.6	-	1.5
18	–355.6	84.2	9.6	0.4	-	-	-	3.0	-	2.2	0.6	3
19	–358.0	94.4	2.2	-	-	-	0.8	1.2	0.6	0.8	-	2
20	–359.2	82.0	16.2	-	-	-	0.4	0.6	0.4	0.4	-	2
21	–362.5	85.8	1.2	-	-	-	0.4	6.0	0.2	5.6	0.8	2.5
22	–363.9	87.4	0.4	-	-	-	0.2	7.0	-	4.6	0.4	2.5
23	–367.3	99.0	1.0	-	-	-	-	<0.1	-	<0.1	-	2.5
24	–370.9	99.2	0.4	-	-	-	-	0.4	-	0.4	-	2
25	–372.6	99.8	0.2	-	-	-	-	<0.1	-	<0.1	-	1.5
26	–376.1	84.8	2.0	-	-	-	-	6.6	-	6.6	-	2
27	–379.5	93.0	0.6	0.2	-	-	0.4	3.6	-	2.2	-	2.5
28	–379.8	92.2	0.8	-	-	-	0.4	3.6	-	3.0	-	3
29	–381.4	75.2	21.2	-	-	-	-	2.0	-	1.6	-	2
30	–383.4	85.0	1.8	1.2	-	-	1.8	5.8	-	4.4	-	2.5
31	–387.6	73.8	23.0	-	-	-	0.2	2.2	-	0.8	-	3
32	–388.2	82.8	16.2	-	-	-	-	0.6	-	0.4	-	3
34	–391.5	79.0	5.8	-	-	-	-	6.2	-	8.6	0.4	2.5
35	–392.0	93.2	6.0	-	-	-	-	0.4	-	0.4	-	2.5
36	–394.4	87.8	11.2	-	-	-	-	0.6	-	0.6	-	2.5
37	–395.8	97.2	2.0	-	-	-	-	-	-	-	0.8	2
38	–398.5	94.8	3.4	1.0	-	-	-	0.8	-	-	-	2.5
39	–403.8	95.8	3.0	0.2	-	-	<0.1	0.4	-	0.6	-	2.5
40	–407.6	95.6	2.6	1.0	-	-	<0.1	0.4	-	0.4	-	2.5
41	–408.8	96.8	0.6	1.2	-	-	0.2	0.6	0.2	0.4	-	2.5
44	–411.3	98.0	1.0	0.4	-	-	0.2	0.2	0.2	0.2	-	2
45	–412.3	98.4	0.2	1.4	-	-	-	-	-	-	-	2
46	–413.6	89.4	0.2	0.2	-	-	2.4	4.6	1.4	1.8	-	2
47	–418.9	87.0	4.0	0.4	-	-	1.8	3.0	1.6	2.2	-	2.5
48	–422.7	93.6	2.0	0.4	-	-	0.8	2.0	-	1.2	-	2.5
49	–426.2	83.6	1.4	1.0	-	-	-	7.0	-	7.0	-	2.5
50	–429.7	93.8	4.2	1.0	-	-	<0.1	0.4	<0.1	0.6	-	2.5
51	–433.9	97.2	1.2	0.2	-	-	0.2	0.8	-	0.4	-	2.5
52	–439.0	58.4	14.0	0.8	-	-	-	13.8	-	13.0	-	2.2
53	–440.4	82.4	11.4	-	-	-	-	2.8	-	3.4	-	2.2
54	–443.8	90.6	0.4	-	-	-	-	6.0	-	2.8	0.2	2
55	–445.8	86.6	0.4	0.4	-	-	1.8	4.6	1.4	4.8	-	2
56	–448.8	75.6	4.2	-	-	-	0.4	11.2	0.2	8.0	0.4	2.5
57	–453.2	75.2	4.0	-	-	-	1.6	10.2	1.2	7.8	-	2.5
59	–456.2	93.0	1.4	-	<0.1	-	2.6	1.0	0.8	-	1.2	2.5
60	–464.5	83.6	1.6	-	<0.1	-	8.0	3.0	1.0	2.8	-	3
61	–469.4	64.6	3.2	-	0.2	-	13.4	5.2	5.8	6.2	1.4	2.5
62	–476.4	65.0	1.6	-	1.8	-	12.6	6.8	5.8	4.4	2.0	1
63	–482.1	72.2	3.0	-	0.4	-	9.6	6.6	2.8	3.0	2.4	2.5
64	–493.6	54.4	9.2	-	4.0	-	15.0	5.8	4.0	6.2	1.4	2.5
65	–495.8	84.8	3.8	-	-	-	1.8	7.0	-	2.6	-	2.5
66	–506.9	80.4	1.4	-	-	-	0.4	10.6	-	5.6	1.6	2.8
67	–511.0	77.4	7.2	-	0.2	-	0.2	10.8	-	3.8	0.4	2.5
68	–514.3	78.8	5.0	-	2.4	-	0.2	8.4	-	4.2	1.0	2.5
69	–521.8	97.4	0.2	-	-	-	-	1.8	-	0.6	-	3
70	–526.0	91.0	3.2	1.0	-	-	0.2	2.0	-	1.2	1.4	2.5

Table 2 (Contd.)

Unit	Depth	Groundmass	Ol		Opx		Plag		Cpx		Opq	A.I.[a]
	(m)	(%, c, m)	Ph	Mph	Ph	Mph	Ph	Mph	Ph	Mph	Mph	(1–5)
71	–526.6	94.2	1.4	1.6	-	-	-	1.8	-	0.6	0.4	2.5
72	–533.8	99.0	0.1	-	-	0.1	-	<0.1	0.2	0.6	-	1.5
73	–535.4	96.6	1.0	0.4	-	-	0.2	1.2	-	0.6	-	2.5
74	–537.9	91.8	0.6	0.2	<0.1	-	-	5.4	0.2	1.8	-	2.5
75	–545.1	95.6	-	-	-	1.2	<0.1	-	-	0.4	2.8	2.5
76	–550.3	90.4	3.8	-	-	-	-	3.6	-	2.2	-	2.5
81	–556.4	96.4	2.2	0.4	-	-	-	0.8	-	0.2	-	2
82	–558.7	90.8	0.4	0.2	-	-	0.2	5.6	<0.1	2.8	-	2.5
83	–562.0	96.6	1.8	-	-	-	-	1.0	-	0.6	-	3
85	–564.9	86.2	10.4	-	-	-	-	2.8	-	0.4	-	4
86	–565.8	87.0	6.6	-	2.4	0.8	<0.1	0.2	1.0	0.8	0.6	4
88	–569.4	72.2	13.6	-	-	-	2.6	8.4	-	3.0	0.2	4
91	–573.7	79.4	4.2	-	-	-	0.2	9.2	0.6	4.8	1.6	3.5
92	–581.9	66.4	33.0	-	<0.1	-	<0.1	0.4	<0.1	<0.1	0.2	3.2
93	–586.4	97.8	0.6	-	-	-	<0.1	1.6	-	<0.1	-	3
94	–590.5	93.2	4.2	-	-	-	-	1.6	-	1.0	-	4
95	–593.7	93.6	1.8	-	-	-	-	3.0	-	1.6	-	4
96	–296.0	93.0	2.0	-	-	-	0.2	3.2	-	1.6	-	4
97	–597.7	74.2	22.2	-	-	-	1.8	0.6	1.2	-	-	4
98	–600.3	97.8	1.8	-	-	-	-	0.4	-	<0.1	-	4
99	–604.6	69.4	30.6	-	-	-	-	-	-	-	-	5
100	–606.3	77.6	0.4	-	-	-	2.6	10.4	<0.1	9.0	-	4
101	–622.4	89.6	2.2	-	-	-	0.2	5.4	-	2.6	-	4
102	–625.5	76.2	8.2	-	-	-	1.2	9.4	-	5.0	-	4
103	–627.8	96.8	1.4	-	-	-	0.2	1.0	-	0.6	-	4

[a]A.I., alteration index, ranging from 1 to 5, increasing with extent of alteration (1, unaltered; 2, thin iddingsite rims on olivine; 3, extensive iddingsite alteration of olivine; 4, matrix altered and vesicles have secondary mineral linings; 5, extensive matrix alteration and total iddingsitization of olivine); ph, phenocrysts; mph, microphenocrysts; opq, opaque phases; ol, olivine; opx, orthopyroxene; plag, plagioclase; cpx, clinopyroxene

Hawaii. Smithsonian natural glass standards VG2 and A99, and mineral standards Durango Apatite (for P; Jarosewich et al. 1979) and orthoclase (K) were used for calibration. A PAP-ZAF correction was applied to all analyses, and minor corrections (<2%) were made based on 5–10 repeated analyses of Smithsonian glasses analyzed both before and after the unknowns. Reported data are an average of 4–28 analyses from each sample, depending on glass abundance. Analytical errors based on counting statistics are within 0.1 wt% for all oxides except SiO_2, CaO, and FeO, which are within 0.25 wt%.

Glass trace element abundances were determined by pulsed laser ablation microsampling, with analysis of the ablation products using an inductively coupled plasma mass spectrometer (LA-ICP-MS). Analyses were conducted at the Australia National University (ANU) according to procedures described in Eggins et al. (1998), using the LAMTRACE data reduction package (Achterbergh et al. 2001).

Geochronology sample selection

The relatively unaltered nature of KSDP flows prompted us to undertake Ar–Ar dating to obtain more accurate dates for the eruption of Ko'olau flows. There were no published Ar–Ar ages for Ko'olau lavas prior to our study, although there are two unpublished Ar–Ar ages for tholeiite bombs from Salt Lake Crater (2.34 ± 0.14 and 2.38 ± 0.36 Ma; D. Woodcock, 2002 personal communication). Strict criteria were applied to the selection of KSDP samples for Ar–Ar dating. Units 14, 19, and 66 were selected based on their relatively unaltered appearance (alteration index < 3 on a scale of 1–5; see Table 2), relatively high K abundance (> 0.4 wt% K_2O), and unaltered geochemistry (K_2O/P_2O_5 > 1.5 and < 0.3 wt% LOI; see below for discussion of these criteria). These samples have a holocrystalline groundmass and < 10% vesicularity. Units 14 and 19 are the least altered units from the top of the core section; unit 66 is one of the least altered flows with relatively high K_2O from the deeper part of the section. Samples were analyzed at the Oregon State University (OSU) geochronology laboratory, using procedures described in Sinton et al. (1996).

Two additional units were selected for age determinations (37 and 75) in an attempt to date paleomagnetic excursions within the KSDP section. Although an attempt was made to select the freshest samples, none of these samples met all sample selection criteria listed above. Unit 37 has relatively low K_2O (0.38 wt%), but is the most holocrystalline lava from a very glassy and highly vesicular portion of the section. Unit 75 also has low K_2O, and a very fine-grained groundmass. These samples were analyzed at

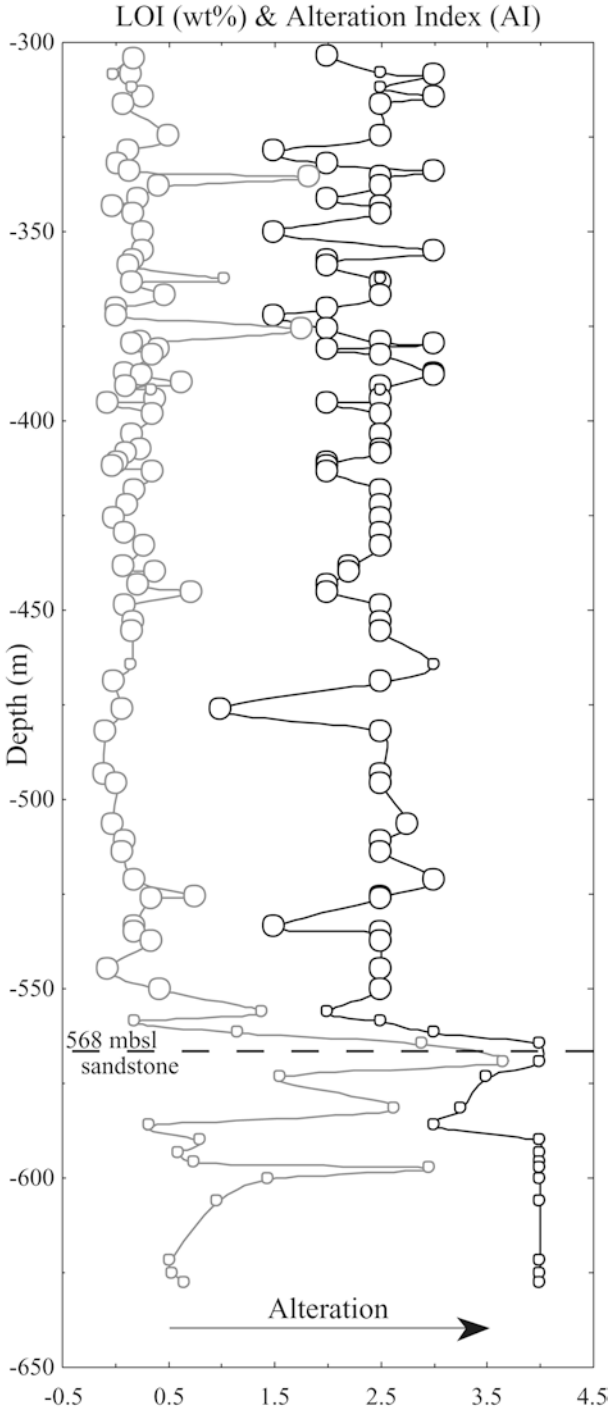

Fig. 3 KSDP core alteration vs. depth. *Smaller symbols* indicate samples with $K_2O/P_2O_5 < 1.2$. Most samples (65 of 72) are unaltered above 551 m b.s.l., indicating that the subsurface lavas on the leeward side of the Ko'olau volcano contain fresh material. Alteration of flows beneath the pebbly sandstone at 568 m b.s.l. may be the result of hydration by a paleostream. Note that all samples with an alteration index (AI) > 3 (see Table 2 for explanation of AI) have $K_2O/P_2O_5 < 1.2$ and high average LOI values. Unit 99 (604.6 m b.s.l.) has an AI of 5 and was not analyzed for LOI

the University of Nevada at the Las Vegas Isotope Geochronology Laboratory according to procedures described in Spell et al. (2003).

Results

Stratigraphy and petrography, KSDP and Wa'ahila Ridge rotary sections

At the top of the KSDP rotary-drilled section, under an 11-m cover of alluvial soil, rock cuttings of nepheline melilitite were recovered from a ~31 m thick depth interval (36 to 5 m a.s.l.; Fig. 2). There is no change in primary mineralogy over this depth interval, although the two deeper samples are more altered and contain calcite (eTable 1; cf. Electronic Supplementary Material). Due to the mixed nature of the rock cuttings and the petrographic similarity of the two Kalihi rejuvenated nepheline melilitites, we were unable to determine whether both of the flows in the valley were sampled.

Ko'olau shield-stage lavas lie directly beneath these Kalihi flows and throughout the Wa'ahila Ridge section (Fig. 2). Rotary drilling obscures flow contacts, making it impossible to determine the exact number of flows intersected within the rotary-drilled depth intervals. Twenty KSDP and 57 Wa'ahila shield-stage flow units were identified by petrographic and geochemical methods, although many more units are probably present within each section but could not be identified using 2–20 mm wide cuttings from sampling intervals of ~3 m. Recent studies (Frey et al. 1994; Jackson et al. 1999) of near-vent flow sequences found average flow thicknesses of 2.1 and 1.6 m, respectively. Cored KSDP flows are thicker (~3.2 m; Table 1), which is consistent with previous measurements (Wentworth and Winchell 1947) of many hundreds of subaerially exposed Ko'olau lavas (~3 m) and the location of KSDP flows ~7.6 km from their caldera source vents. Using this 3.2-m KSDP average flow thickness, the 308-m-thick rotary-drilled KSDP section may represent ~96 Ko'olau flows, and the 432.8-m-thick Wa'ahila section ~135 flows.

Olivine is the dominant phenocryst phase in the KSDP rotary section and Wa'ahila lavas, although some KSDP rock fragments contain only phenocrysts of orthopyroxene and/or plagioclase (eTables 1 and 2). Many olivine phenocrysts are skeletal, indicating rapid cooling (Donaldson 1976). Even in the freshest sections olivine is slightly altered, with thin iddingsite rims < 0.2 mm. Olivine in some lavas is dark in color from minute iron oxide inclusions, indicative of baking (Haggerty and Baker 1967).

Plagioclase is common in the chips recovered from both drill holes, occurring as unaltered phenocrysts, microphenocrysts, and in the groundmass. Phenocrysts of plagioclase are normally more abundant than pyroxene but are usually subordinate to olivine. They are common in the bottom of the KSDP rotary section (particularly from 250 to 300 m b.s.l.). Most crystals are subhedral and occur either as isolated crystals or in clusters with pyroxene.

The presence of orthopyroxene (opx) is typical of Ko'olau basalts, and thought to be the result of their

high SiO_2 compared to other Hawaiian volcanoes (Wentworth and Winchell 1947). For example, opx phenocrysts occur in 27 of the 35 Ko'olau basalts (77%) sampled at WAFB (Takahashi and Takeguchi, unpublished data). Opx phenocrysts or microphenocrysts are present in 18 of 28 KSDP and 15 of 37 Wa'ahila distinct rock chips examined in thin sections (eTables 1 and 2). Opx is found in 82% of the flows from the upper part of the Wa'ahila (above 136 m b.s.l.), whereas clinopyroxene (cpx) occurs in < 10% of these flows (eTable 2). In contrast, cpx occurs in 58% of the underlying Wa'ahila flows but only 23% of these flows contain opx (eTable 2). In the KSDP section below 215 m b.s.l. orthopyroxene is rare to absent. Opx and cpx occur as isolated crystals up to 8 mm in diameter (most are small, 0.3–0.8 mm), or as glomerocrysts with plagioclase and cpx. Clinopyroxene is present only as microphenocrysts and in the groundmass of KSDP rotary section lavas, although it occurs as a phenocryst in the lower Wa'ahila section (at and below 136 m b.s.l.).

Opaque phases are present in the lavas from both drill holes. They occur as small equant microphenocrysts (0.1–0.2 mm) or as tiny inclusions in olivine. They appear fresh in thin section.

KSDP cored section

Core recovery for KSDP was excellent (~95%), revealing 103 subaerially erupted lava flows and one sedimentary unit (Table 1, Fig. 3). Pāhoehoe is overwhelmingly the dominant flow type both in percent of section and number of flows, including two intervals in the middle of the section containing 12 and 13 consecutive pāhoehoe units. 'A'ā and pāhoehoe units have virtually the same average flow thickness (~3 m); the two massive units are thicker (~5 m; Table 1). Fresh, glassy contacts between pāhoehoe units indicate that they were inflated during emplacement or are compound flows composed of multiple lobes. Of the 103 flows, 68 are basalts (< 5 vol% olivine), 22 are olivine basalts (5–15 vol% olivine), and 13 are picritic flows (> 12 wt% MgO and > 15 vol% olivine). The two massive flows are both picritic; otherwise basalts are the dominant lithology regardless of flow type. A thin (~1 m) pebbly sandstone unit was recovered at 566 m b.s.l. in the section. Most of these pebbles are grains of olivine, orthopyroxene, clinopyroxene, and plagioclase occurring in both fresh and altered states. Most flows above the sandstone appear unaltered or weakly altered; below it, all of the flows are moderately to strongly altered (Table 2).

Phenocrysts of olivine, plagioclase, and clinopyroxene are common in the KSDP core, while orthopyroxene phenocrysts are relatively rare (present in 16.5% of lavas) compared to the rotary-drilled section (61.5%). Olivine is usually the most abundant phenocryst phase, and textural relationships indicate that it was the first to crystallize. Many olivine phenocrysts exhibit skeletal growth. In addition, many flows contain numerous olivine xenocrysts that were oxidized by baking. The amount of olivine iddingsitization was used as an indicator of the extent of alteration (Table 2). In the more

Table 3 Results from ^{40}Ar–^{39}Ar radiometric dating

Depth (m b.s.l.)	Unit	Incremental heating (°C)	Plateau age ± 2σ (Ma)	^{39}Ar (%)	MSWD	Normal isochron age ± 2σ (Ma)	$^{40}Ar/^{36}Ar_i \pm 2\sigma$[b]	MSWD	Inverse isochron age ± 2σ (Ma)	$^{40}Ar/^{36}Ar_i \pm 2\sigma$	MSWD[c]
341.9	14	600[a]									
		700[a]									
		800[a]									
		950[a]	2.89 ± 0.12	82.0	0.73	2.89 ± 0.55	295.4 ± 12.3	1.16	2.90 ± 0.53	295.3 ± 11.8	1.09
		1,100									
		1,250									
		1,400									
357.8	19	600[a]									
		750[a]									
		850[a]									
		950[a]	2.83 ± 0.16	88.0	0.06	2.73 ± 0.74	297.8 ± 17.0	0.05	2.72 ± 0.74	297.8 ± 16.9	0.05
		1,100									
		1,250									
		1,400									
506.9	66	600[a]									
		800[a]									
		900[a]									
		1,000[a]	2.90 ± 0.22	97.7	0.89	2.98 ± 0.55	294.4 ± 6.3	1.12	3.00 ± 0.53	294.4 ± 6.2	1.07
		1,100[a]									
		1,250[a]									
		1,400									

[a]Heating steps used in the plateau and isochron age calculations
[b]Initial $^{40}Ar/^{36}Ar$ based on the inverse of the y-intercept of the regression
[c]MSWD (mean square of weighted deviates) describes how well the data are fit by the isochron; a perfect-fit MSWD = 1

Table 4 XRF whole-rock, major element analyses for KSDP and Wa'ahila Ridge lavas. All values are in weight %

Unit	Elev. (m)	SiO_2	TiO_2	Al_2O_3	Fe_2O_3*[b]	MnO	MgO	CaO	Na_2O	K_2O	P_2O_5	Total	LOI
Tunnel flow													
Alt.[a]	~50	52.31	1.77	13.68	11.46	0.16	8.88	8.81	2.56	0.12	0.22	99.99	1.27
KSDP rotary-drilled section													
Alt.	0.4	52.48	1.67	13.79	10.98	0.16	8.63	8.90	2.54	0.23	0.22	99.59	-
	−62.9	52.11	2.24	14.56	11.49	0.15	6.25	9.41	2.71	0.38	0.32	99.62	-
	−88.8	52.36	2.07	14.57	11.17	0.15	6.43	10.00	2.74	0.40	0.29	100.17	-
Alt.	−181.8	49.06	2.33	14.62	12.33	0.16	7.82	10.61	2.36	0.11	0.30	99.70	-
	−209.2	52.67	1.80	13.20	11.05	0.16	8.88	8.81	2.45	0.43	0.25	99.69	-
Alt.	−212.3	50.30	2.25	14.60	11.95	0.17	7.65	10.59	2.36	0.14	0.29	100.30	0.11
	−215.3	53.60	1.89	14.03	10.65	0.15	7.10	9.25	2.61	0.44	0.26	99.98	0.19
Alt.	−218.4	50.05	2.32	14.56	12.38	0.18	7.48	10.72	2.39	0.23	0.31	100.61	1.13
Alt.	−221.4	50.41	2.30	14.40	12.23	0.18	7.29	10.64	2.32	0.11	0.32	100.18	0.80
Alt.	−224.5	50.37	2.28	14.72	12.10	0.18	7.20	10.50	2.25	0.12	0.29	100.00	1.56
Alt.	−227.5	51.30	2.19	14.01	11.71	0.17	7.31	10.45	2.39	0.23	0.26	100.02	0.28
Alt.	−230.6	48.99	2.70	15.10	12.22	0.17	7.00	10.78	2.40	0.24	0.35	99.94	0.79
Alt.	−233.6	50.97	2.25	14.47	11.95	0.17	7.36	10.61	2.31	0.15	0.25	100.49	0.48
Alt.	−236.7	50.87	2.33	14.44	12.03	0.17	6.92	10.57	2.42	0.16	0.26	100.17	0.67
Alt.	−244.3	49.94	2.47	14.21	12.31	0.17	7.18	10.68	2.49	0.20	0.27	99.92	-
Alt.	−268.7	49.07	2.25	12.83	12.55	0.18	10.21	9.96	2.13	0.19	0.25	99.61	-
	−303.7	50.75	2.31	13.33	12.27	0.18	7.95	10.23	2.23	0.34	0.26	99.85	-
KSDP cored section													
1	−303.8	49.34	1.59	11.32	11.72	0.17	15.42	8.20	1.94	0.27	0.18	100.15	0.16
2[a]	−308.4	48.14	1.36	9.87	12.30	0.17	18.62	7.23	1.65	0.15	0.16	99.64	−0.02
3	−308.9	49.27	1.54	10.95	11.83	0.17	15.95	7.95	1.83	0.26	0.18	99.92	0.16
4[a]	−312.3	51.78	1.85	13.28	11.12	0.16	9.52	9.29	2.33	0.23	0.21	99.77	0.16
5	−314.4	50.36	1.56	11.37	11.50	0.16	14.55	7.90	1.91	0.22	0.19	99.71	0.26
6	−316.6	50.14	1.54	11.22	11.53	0.16	15.07	7.87	1.89	0.29	0.18	99.90	0.09
7	−325.0	50.35	1.98	12.54	11.91	0.17	10.65	9.45	1.93	0.38	0.20	99.58	0.50
8	−329.0	50.40	1.97	12.08	11.86	0.17	11.53	9.25	2.11	0.38	0.23	99.98	0.13
9	−332.4	52.60	1.70	13.22	11.34	0.17	9.19	9.18	2.38	0.26	0.17	100.21	0.03
10	−334.2	52.10	1.71	13.22	11.36	0.17	9.07	9.20	2.35	0.21	0.16	99.53	0.14
12[a]	−336.0	52.12	1.70	13.12	11.42	0.17	9.41	9.13	2.35	0.30	0.16	99.88	1.83
13	−338.0	50.79	2.34	13.48	12.22	0.18	7.82	10.47	2.22	0.50	0.27	100.28	0.41
14	−341.9	50.65	2.33	13.43	12.15	0.17	7.92	10.46	2.30	0.51	0.28	100.20	0.22
15	−343.8	50.97	2.02	12.86	12.28	0.17	9.49	9.62	2.20	0.40	0.22	100.23	−0.02
16	−345.5	50.35	2.50	13.46	12.44	0.17	7.46	10.69	2.02	0.45	0.28	99.83	0.17
17	−350.4	50.97	2.30	13.75	12.05	0.17	7.51	10.49	2.23	0.42	0.25	100.13	0.26
18	−355.6	50.30	2.36	13.81	12.20	0.17	7.31	10.70	2.23	0.43	0.27	99.78	0.27
19	−357.8	50.88	2.44	13.86	12.07	0.17	7.05	10.76	2.30	0.52	0.29	100.33	0.17
20	−359.2	49.13	1.94	11.47	12.28	0.17	13.66	8.95	1.85	0.44	0.22	100.12	0.13
21[a]	−362.5	51.30	2.30	14.36	11.82	0.17	6.89	10.30	2.17	0.18	0.20	99.69	1.03
22	−363.9	52.25	2.09	14.11	11.15	0.17	7.15	10.45	2.37	0.38	0.24	100.36	0.16
23	−367.3	52.07	2.15	13.95	11.66	0.18	7.20	10.13	2.28	0.36	0.21	100.17	0.47
24	−370.6	52.20	2.13	13.74	11.64	0.17	7.18	10.05	2.42	0.37	0.23	100.12	0.01
25	−372.5	51.93	2.13	13.79	11.70	0.17	7.26	10.10	2.38	0.32	0.22	100.00	0.01
26[a]	−376.1	51.62	2.24	13.67	11.76	0.17	7.53	10.37	2.29	0.43	0.25	100.32	1.76
27	−379.5	51.76	2.22	14.09	11.34	0.17	6.88	10.55	2.35	0.32	0.24	99.91	0.24
28	−379.8	51.96	2.25	14.05	11.33	0.17	6.58	10.48	2.29	0.45	0.25	99.79	0.16
29	−381.3	49.21	1.91	12.03	12.42	0.18	12.81	9.06	2.00	0.31	0.20	100.13	0.41
30	−383.0	50.59	1.97	12.32	12.05	0.18	11.39	9.28	1.98	0.28	0.23	100.27	0.36
31	−387.6	46.89	1.34	8.49	13.19	0.18	21.74	6.47	1.57	0.20	0.14	100.20	0.09
32	−388.2	49.30	1.91	11.97	12.37	0.18	12.73	8.98	2.06	0.22	0.19	99.92	0.25
33	−390.0	50.47	2.23	13.41	12.10	0.18	8.77	10.26	2.05	0.27	0.20	99.92	0.63
34	−391.4	50.48	2.14	12.96	12.13	0.18	9.64	10.07	2.22	0.28	0.20	100.31	0.11
35[a]	−392.0	51.25	2.24	13.32	11.96	0.18	8.48	10.25	2.13	0.25	0.24	100.29	0.34
36	−394.4	49.67	2.10	12.64	12.58	0.19	10.55	9.72	2.10	0.25	0.18	99.97	0.38
37	−395.8	50.85	2.25	13.52	12.00	0.18	8.07	10.67	2.22	0.38	0.25	100.37	−0.07
38	−398.6	51.21	2.32	13.50	12.11	0.18	7.60	10.59	2.23	0.31	0.22	100.27	0.35
39	−403.8	50.66	2.42	13.45	12.49	0.18	7.62	10.72	2.17	0.38	0.23	100.31	0.16
40	−407.6	50.46	2.34	13.24	12.43	0.18	8.05	10.58	2.18	0.36	0.22	100.04	0.24
41	−408.8	50.63	2.39	13.41	12.34	0.18	7.38	10.72	2.34	0.32	0.23	99.94	0.11
44	−411.2	50.76	2.38	13.54	12.24	0.18	7.35	10.75	2.31	0.40	0.24	100.15	0.03
45	−412.3	50.25	2.06	12.19	12.17	0.18	11.04	9.35	2.14	0.40	0.22	100.00	−0.02
46	−413.6	51.36	2.26	13.61	11.68	0.17	7.58	10.44	2.43	0.38	0.23	100.14	0.36
47	−418.8	51.24	2.22	13.59	11.58	0.18	7.46	10.41	2.42	0.41	0.24	99.74	0.18
48	−422.7	51.58	2.29	13.82	11.53	0.17	6.87	10.59	2.71	0.44	0.25	100.25	0.12
49	−426.1	51.25	2.18	13.62	11.79	0.18	7.41	10.65	2.47	0.34	0.21	100.09	−0.01

Table 4 (Contd.)

Unit	Elev. (m)	SiO_2	TiO_2	Al_2O_3	Fe_2O_3*[b]	MnO	MgO	CaO	Na_2O	K_2O	P_2O_5	Total	LOI
50	−429.7	51.02	2.10	12.68	11.82	0.17	9.79	9.51	2.45	0.38	0.22	100.14	0.09
51	−433.4	51.45	2.25	13.77	11.64	0.17	7.56	10.40	2.31	0.36	0.20	100.13	0.28
52	−438.9	49.74	1.97	12.33	11.85	0.18	11.36	9.25	2.31	0.33	0.21	99.53	0.08
53	−440.4	50.09	1.95	12.25	11.90	0.18	12.02	8.94	2.31	0.37	0.20	100.20	0.38
54	−443.7	51.25	2.40	13.78	11.80	0.18	6.95	10.72	2.53	0.40	0.25	100.26	0.22
55	−445.7	49.65	2.52	14.28	12.16	0.18	6.92	11.01	2.49	0.22	0.17	99.59	0.72
56	−448.8	50.94	2.33	13.92	11.69	0.18	7.04	10.93	2.60	0.32	0.25	100.20	0.09
57	−453.2	51.05	2.35	13.77	11.89	0.18	7.37	10.60	2.44	0.36	0.23	100.23	0.17
59	−456.1	51.36	2.39	13.73	11.74	0.17	7.12	10.55	2.51	0.49	0.26	100.32	0.16
60[a]	−464.5	50.88	2.54	14.03	12.01	0.18	6.45	10.29	2.68	0.27	0.25	99.58	0.15
61	−469.3	51.27	2.29	13.79	11.71	0.17	7.34	10.23	2.57	0.42	0.25	100.04	−0.01
62	−476.4	50.93	2.23	12.98	11.97	0.18	8.68	10.23	2.33	0.38	0.23	100.12	0.07
63	−482.1	51.57	2.31	13.66	11.66	0.17	6.90	10.34	2.57	0.47	0.25	99.90	−0.09
64	−493.4	51.66	1.67	12.61	11.51	0.17	10.76	9.28	2.30	0.25	0.16	100.38	−0.10
65	−495.9	51.19	1.95	12.49	11.81	0.17	10.02	9.47	2.36	0.34	0.21	100.01	0.01
66	−506.9	51.23	2.09	13.03	11.48	0.17	8.60	9.92	2.46	0.42	0.22	99.63	−0.02
67	−511.0	51.89	1.87	13.15	11.35	0.17	8.78	9.42	2.62	0.31	0.17	99.71	0.09
68	−514.2	50.80	1.98	12.84	11.69	0.17	10.09	9.39	2.48	0.26	0.18	99.89	0.07
69	−521.8	52.29	2.03	13.91	11.13	0.18	7.02	10.00	2.74	0.29	0.17	99.75	0.19
70	−526.0	52.35	2.00	13.90	11.53	0.17	8.02	9.73	2.24	0.25	0.13	100.32	0.76
71	−526.5	51.97	2.06	13.71	11.56	0.18	8.17	10.02	2.17	0.31	0.15	100.28	0.34
72	−533.7	52.18	2.17	13.89	11.39	0.17	7.20	10.33	2.32	0.27	0.23	100.15	0.18
73	−535.2	51.24	2.23	13.95	11.50	0.17	7.06	10.54	2.59	0.27	0.22	99.77	0.19
74	−537.9	52.15	2.14	13.95	11.44	0.17	7.23	10.33	2.25	0.31	0.18	100.14	0.35
75	−544.9	51.72	2.18	13.70	11.60	0.18	7.21	10.32	2.30	0.36	0.23	99.79	−0.07
76	−550.3	48.66	2.32	13.25	12.44	0.19	9.62	10.68	2.34	0.18	0.12	99.78	0.43
81[a]	−556.4	49.66	2.25	14.47	11.98	0.17	7.64	10.39	2.46	0.38	0.09	99.49	1.38
82[a]	−558.7	50.37	2.29	13.98	11.95	0.18	7.11	10.73	2.65	0.19	0.23	99.67	0.19
83[a]	−562.0	49.39	2.30	14.36	12.30	0.18	7.72	10.99	2.22	0.19	0.21	99.85	1.15
85[a]	−564.8	50.06	2.17	14.07	12.18	0.16	8.50	9.72	2.26	0.24	0.19	99.55	2.89
88[a]	−569.4	48.89	1.80	12.60	12.46	0.26	13.02	8.19	2.03	0.19	0.17	99.61	3.65
91[a]	−573.7	49.22	2.57	13.81	12.28	0.19	8.34	11.20	2.09	0.19	0.27	100.14	1.55
92[a]	−581.7	46.63	1.58	9.22	12.62	0.19	21.11	6.68	1.59	0.14	0.17	99.95	2.63
93[a]	−586.4	50.62	2.33	14.18	11.68	0.18	7.12	10.93	2.6	0.15	0.24	100.03	0.33
94[a]	−590.4	51.21	2.17	13.71	11.06	0.17	8.46	10.43	2.42	0.14	0.21	99.99	0.80
95[a]	−593.7	50.65	2.21	13.75	11.50	0.17	8.21	10.55	2.45	0.20	0.19	99.87	0.60
96[a]	−596.0	51.34	2.03	13.79	10.81	0.17	8.26	10.64	2.34	0.12	0.21	99.70	0.74
97[a]	−597.7	47.24	2.12	11.21	13.02	0.20	15.63	8.96	1.37	0.13	0.22	100.09	2.95
98[a]	−600.3	48.75	2.39	13.80	12.22	0.18	8.75	11.12	2.15	0.16	0.20	99.71	1.44
100[a]	−606.3	50.20	2.29	13.86	12.00	0.18	7.72	11.44	2.05	0.21	0.24	100.18	0.96
101[a]	−622.3	50.78	2.01	13.69	11.17	0.17	8.21	10.95	2.43	0.18	0.20	99.79	0.52
102[a]	−625.5	50.80	2.19	13.32	11.73	0.18	7.98	10.63	2.38	0.22	0.21	99.63	0.54
Wa'ahila Ridge cuttings													
Alt.	−59.4	50.90	2.26	14.72	11.79	0.15	7.04	10.03	1.92	0.28	0.26	99.35	2.37
	−80.8	51.82	2.20	14.22	11.40	0.16	6.70	9.99	2.38	0.41	0.28	99.56	0.20
Alt.	−108.2	52.13	2.14	14.49	11.34	0.16	6.79	9.75	2.54	0.28	0.30	99.93	0.23
Alt.	−163.1	49.03	2.40	14.32	12.22	0.17	8.50	10.49	1.95	0.26	0.29	99.62	7.87
	−198.1	51.03	2.33	13.73	11.84	0.17	7.98	10.00	2.00	0.41	0.27	99.75	0.32
	−205.7	51.50	2.11	13.55	11.23	0.16	8.05	9.90	2.25	0.48	0.25	99.48	0.73
	−236.2	51.79	2.22	13.71	11.37	0.17	7.37	10.26	2.15	0.49	0.25	99.79	0.56
	−263.7	50.84	2.52	14.16	11.22	0.16	6.66	10.75	2.52	0.54	0.29	99.66	0.42
	−278.9	51.89	2.28	14.03	11.62	0.17	6.21	10.49	2.25	0.41	0.25	99.59	0.42
	−306.3	51.03	2.07	13.36	11.76	0.18	8.86	9.84	2.11	0.35	0.21	99.78	0.52
	−318.5	50.48	1.78	12.04	11.67	0.22	12.19	9.01	1.76	0.26	0.17	99.58	0.27
Alt.	−330.7	50.20	2.32	12.81	12.10	0.17	9.32	10.24	1.85	0.25	0.22	99.48	0.59

[a]Alt., altered samples ($K_2O/P_2O_5 < 1.2$ or > 2.2 and/or LOI > 0.8) are not shown in geochemical variation diagrams
[b]Total iron as Fe_2O_3; -, no data

altered flows at the bottom of the cored section (550–630 m b.s.l.), olivine is almost completely replaced by iddingsite.

Orthopyroxene is unevenly distributed with depth. It is present as phenocrysts in six of the upper 11 cored units (304–336 m b.s.l.) but it is absent in the underlying 39 flows (~100 m). In the bottom section of the KSDP hole, orthopyroxene occurs sporadically (seven of 40 flows) and always at < 2 vol% (Table 2). Where present, orthopyroxene almost always contains olivine inclusions, and commonly has a thin rim (~0.1 mm) of clinopyroxene. Plagioclase is common in the KSDP core, second in abundance as a phenocryst only to olivine. Plagioclase is present in variable amounts

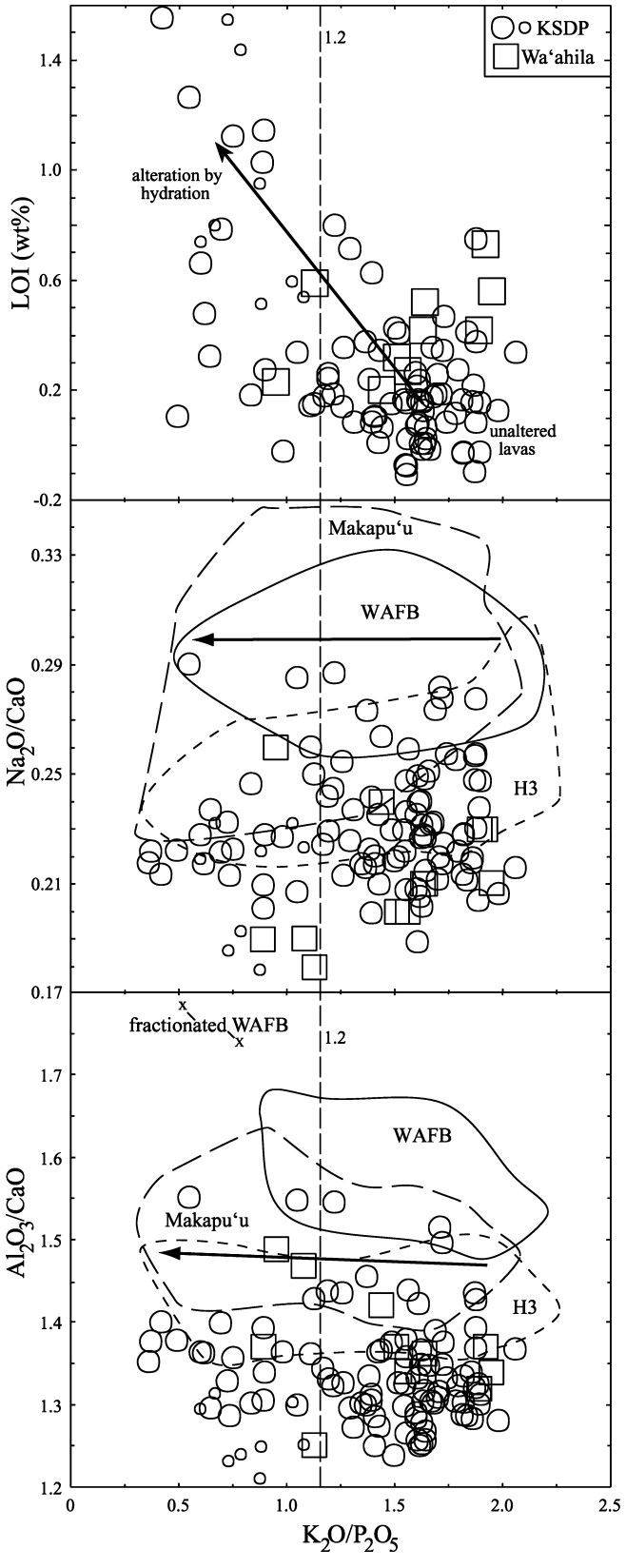

Fig. 4 K_2O/P_2O_5 plots for evaluating whole-rock alteration effects on shield-stage Ko'olau lavas. Samples with *small symbols* have AI > 3. Data for the Wheeler Air Force Base (*WAFB*) are from Takeguchi and Takahashi (unpublished data), for Makapu'u from Frey et al. (1994), and for H3 from Jackson et al. (1999). The *arrow* indicates the effect of alteration, which is to lower K_2O/P_2O_5 with little or no effect on Al_2O_3/CaO. The two WAFB samples (*x*) with high Al_2O_3/CaO are strongly fractionated (< 6 wt% MgO). Ten KSDP rotary section lavas are not shown due to an insufficient amount of sample material for LOI analysis. Six of these samples have $K_2O/P_2O_5 < 1.2$. While K_2O/P_2O_5 generally decreases and LOI increases with increasing alteration, other geochemical characteristics are also affected

(0–14%) as unaltered phenocrysts and microphenocrysts, and is always present in the groundmass (Table 2). Phenocrysts and/or microphenocrysts of plagioclase occur in clusters with clinopyroxene of the same size, and the two minerals occur in similar abundances (Table 2), indicating that these two phases crystallized simultaneously.

The common presence of clinopyroxene phenocrysts (30 of the 90 examined litholigic units) in the KSDP core is a striking petrographic feature compared to the overlying rotary-drilled section (eTable 1) and surface Ko'olau lavas. The presence of clinopyroxene and its dominance over opx in the lower parts of both holes indicates earlier crystallization of this phase than in typical Ko'olau lavas, suggesting that lower KSDP lavas are geochemically distinct from subaerially exposed Ko'olau flows.

Geochronology

Published K–Ar dates for Ko'olau lavas are commonly inconsistent, even from a single site (e.g., ages from individual flows may vary up to 1 Ma (Doell and Dalrymple 1973), due to leaching of potassium in surface Ko'olau lavas by tropical weathering (Frey et al. 1994). The most reliable K–Ar age determinations for this volcano range from 1.8 to 2.7 Ma (McDougall 1964, Doell and Dalrymple 1973; Lanphere and Dalrymple 1980), although the youngest ages were determined on samples with very low K_2O (0.109–0.135 wt%) and low radiogenic ^{40}Ar (nine of 10 samples have < 8% radiogenic ^{40}Ar; Doell and Dalrymple 1973). Paleomagnetic analyses of Ko'olau lavas (Doell and Dalrymple 1973) generally show reversed polarity, which is consistent with their eruption in the Matuyama epoch (2.58–0.78 Ma; Cande and Kent 1995). However, rare flows have been found with normal polarity (Herrero-Bervera et al. 2002), and are thought by these workers to have been erupted during one of the two Réunion subchrons (2.11–2.15 Ma; McDougall et al. 1992), based on the ages of nearby lavas dated by Doell and Dalrymple (1973). The oldest Ko'olau K–Ar age (2.7 ± 0.2 Ma; Doell and Dalrymple 1973) is from a section of reversely polarized lavas; therefore, its age is likely to be < 2.58 Ma.

KSDP units 14, 19, and 66 all produced flat plateaus for 82–98% of released argon. The initial $^{40}Ar/^{36}Ar$ values for these samples by normal and inverse isochron

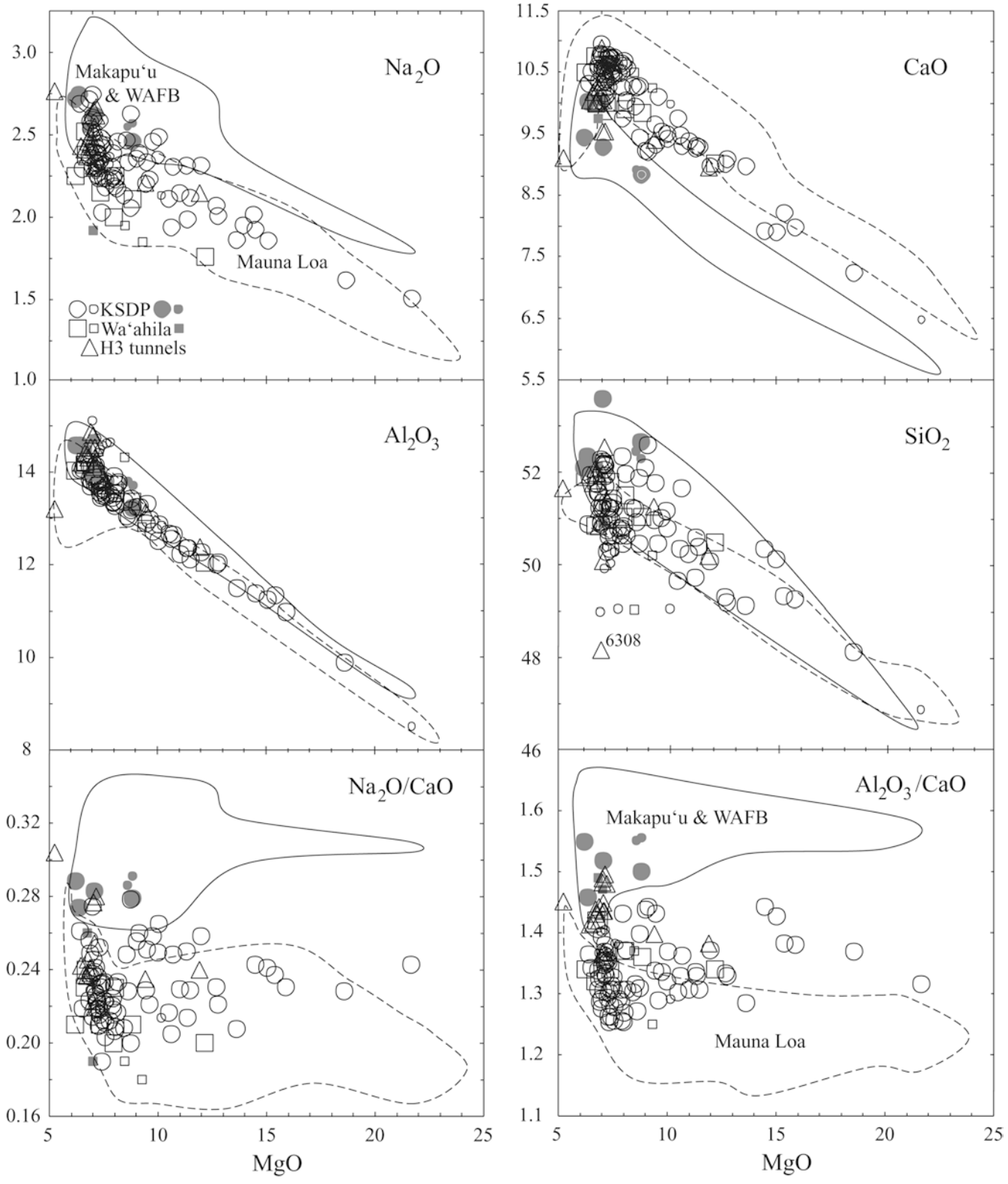

Fig. 5 Whole-rock MgO variation diagrams for KSDP and Wa'ahila lavas. *Symbols* as in Fig. 4, except *small open squares* for altered Wa'ahila Ridge lavas ($K_2O/P_2O_5 < 1.2$) and *solid symbols* for geochemically distinct samples from the rotary sections. The *solid line* encloses surface and shallow Ko'olau lavas from Makapu'u (Frey et al. 1994; 31 analyses) and the WAFB core (Takeguchi and Takahashi, unpublished data; 24 analyses). The *dashed border* encloses Mauna Loa analyses (data from J.M. Rhodes, personal communication 2002; 158 analyses). All analyses except WAFB are from the same laboratory (University of Massachusetts), thereby minimizing interlaboratory bias in this comparison. Note that Ko'olau and Mauna Loa lavas with > 8.0 wt% MgO are distinct for Na_2O and CaO, and that KSDP rocks are more similar to those of Mauna Loa for these oxides. H3 tunnel samples (Jackson et al. 1999) have compositions between those of typical Ko'olau and Mauna Loa lavas. Analytical error is less than the size of *large symbols*

Table 5 XRF whole-rock, trace element analyses in ppm for KSDP lavas

Unit	Elev. (m)	V	Cr	Ni	Zn	Rb	Sr	Y	Zr	Nb	Ba	Ce
Tunnel flow												
	~50	204	551	239	111	0.8	317	21.4	109	6.6	111	19
Cored section												
1	−303.8	193	746	596	104	3.0	267	17.7	101	7.0	64	19
2	−308.4	175	797	769	109	1.7	235	15.3	86	6.0	66	19
3	−308.9	183	717	594	105	3.4	256	17.2	96	6.6	61	20
4	−312.3	205	608	234	104	2.5	324	20.2	121	7.5	72	25
5	−314.4	175	801	576	105	2.4	272	17.4	102	6.2	72	17
6	−316.6	179	794	588	104	3.6	272	17.3	101	6.1	63	19
7	−325.0	229	718	315	110	4.4	302	20.9	126	8.0	70	21
8	−329.0	225	638	361	104	4.7	308	21.6	127	8.1	69	26
9	−332.4	193	478	163	98	3.5	268	20.6	104	6.5	56	18
10	−334.2	200	517	166	103	2.0	266	20.0	104	6.7	64	19
12	−336.0	208	504	164	103	3.3	267	19.9	106	6.8	63	19
13	−338.0	257	341	105	108	6.8	374	23.7	154	10.5	94	28
14	−341.9	257	331	102	106	7.1	377	24.0	154	10.5	94	33
15	−343.8	236	522	210	108	5.4	307	21.7	127	9.3	85	25
16	−345.5	268	337	103	106	6.6	392	24.3	161	11.5	103	30
17	−350.4	254	348	104	112	5.7	351	23.7	143	10.4	90	24
18	−355.6	254	284	102	107	5.6	380	24.2	153	10.8	86	32
19	−357.8	259	277	82	105	6.2	382	24.7	157	11.0	96	29
20	−359.2	225	735	471	107	5.4	307	20.1	128	9.3	82	26
21	−362.5	246	260	75	108	1.6	355	23.3	148	10.1	103	27
22	−363.9	231	289	78	98	5.0	352	22.4	133	8.9	86	27
23	−367.3	237	333	80	108	4.4	334	23.7	138	9.3	79	29
24	−370.6	241	291	79	106	4.8	337	23.6	139	9.1	74	26
25	−372.5	238	279	80	106	3.9	335	23.2	137	9.1	84	25
26	−376.1	238	289	93	101	5.7	353	24.1	145	9.5	86	29
27	−379.5	238	298	88	103	4.2	355	24.1	144	9.6	84	28
28	−379.8	237	288	84	106	6.0	351	23.5	147	9.9	87	27
29	−381.3	222	756	388	110	3.9	305	20.6	126	8.4	71	24
30	−383.0	217	734	331	108	4.5	311	22.2	129	8.7	87	25
31	−387.6	159	938	973	110	1.8	219	14.3	88	5.8	60	18
32	−388.2	213	776	392	111	2.3	305	19.9	124	8.2	75	26
33	−390.0	239	525	177	110	3.7	318	22.7	138	9.5	84	27
34	−391.4	234	512	194	99	3.5	322	22.6	135	9.2	85	25
35	−392.0	240	495	157	109	3.0	323	24.4	140	9.4	87	24
36	−394.4	235	602	243	113	2.9	308	21.7	132	8.9	82	25
37	−395.8	256	404	126	109	4.5	336	24.0	142	9.7	82	28
38	−398.6	246	377	116	107	4.7	336	23.8	146	10.0	86	25
39	−403.8	268	363	103	113	4.4	337	24.7	151	10.4	90	29
40	−407.6	241	421	125	111	4.3	329	24.2	146	10.2	78	25
41	−408.8	241	340	91	108	3.7	337	25.8	149	10.3	82	22
44	−411.2	250	323	82	105	4.4	337	24.9	150	10.4	86	27
45	−412.3	227	710	282	107	4.4	309	21.9	133	9.0	74	25
46	−413.6	249	338	112	112	5.0	348	23.1	144	9.9	101	28
47	−418.8	249	311	109	100	5.2	351	23.2	143	9.7	85	30
48	−422.7	248	267	78	104	5.5	355	23.6	148	10.4	87	28
49	−426.1	233	316	97	97	4.3	334	22.7	138	9.2	71	28
50	−429.7	218	519	188	106	4.8	358	21.0	141	10.0	104	26
51	−433.4	249	366	100	102	4.8	343	23.5	144	9.1	77	27
52	−438.9	222	492	342	108	4.4	318	21.0	127	9.3	86	25
53	−440.4	197	473	364	104	5.0	308	20.3	125	9.0	91	23
54	−443.7	244	263	78	103	5.4	369	24.7	153	11.5	112	29
55	−445.7	263	253	82	115	2.6	375	24.4	159	12.2	106	30
56	−448.8	249	268	81	108	4.6	373	23.8	149	11.3	116	28
57	−453.2	234	290	92	105	5.0	366	23.6	150	11.2	114	30
59	−456.1	235	292	86	104	6.3	361	24.5	151	11.2	102	28
60	−464.5	248	228	84	109	2.6	366	26.3	160	12.6	119	28
61	−469.3	237	323	113	97	5.9	354	23.7	144	11.0	101	30
62	−476.4	231	415	148	100	5.8	331	22.2	129	10.2	104	28
63	−482.1	238	290	91	99	6.7	347	24.2	143	11.2	105	29
64	−493.4	197	585	253	94	3.6	267	18.9	98	6.6	64	20
65	−495.9	216	576	232	98	4.7	296	21.0	118	7.9	75	24
66	−506.9	223	446	160	97	5.4	320	22.0	131	9.2	79	26
67	−511.0	205	427	133	98	4.0	293	20.6	116	7.7	65	20
68	−514.2	214	532	240	104	3.2	322	21.4	126	8.2	80	26

Table 5 (Contd.)

Unit	Elev. (m)	V	Cr	Ni	Zn	Rb	Sr	Y	Zr	Nb	Ba	Ce
69	−521.8	227	295	87	102	4.5	304	23.6	126	8.2	75	22
70	−526.0	213	355	118	107	2.7	307	21.0	122	8.0	283	22
71	−526.5	223	345	123	101	4.3	312	22.6	128	8.5	82	23
72	−533.7	234	254	80	99	3.0	322	23.8	136	9.1	77	22
73	−535.2	244	300	82	106	3.5	332	24.3	143	9.4	92	26
74	−537.9	234	297	78	103	4.3	327	22.7	136	8.8	99	24
75	−544.9	223	309	72	97	5.6	320	23.8	138	8.9	81	25
76	−550.3	270	542	215	112	1.9	308	22.0	139	9.1	84	26
81	−556.4	256	342	130	117	8.9	318	24.0	141	9.6	226	24
82	−558.7	242	266	84	106	2.1	334	26.1	143	9.2	86	30
83	−562.0	267	336	133	116	2.4	335	26.3	144	9.6	65	29
85	−564.8	234	477	210	135	2.8	281	23.4	132	10.7	114	28
88	−569.4	176	615	436	109	3.0	222	19.0	104	8.2	108	23
91	−573.7	278	395	149	117	2.4	378	25.2	166	13.9	159	39
92	−581.7	174	995	912	114	2.1	188	16.3	94	7.7	287	17
93	−586.4	264	317	101	107	1.9	332	24.7	143	9.7	119	26
94	−590.4	244	472	184	114	1.3	332	23.4	127	8.3	65	23
95	−593.7	247	439	171	103	1.6	330	23.1	130	8.7	56	25
96	−596.0	237	469	165	111	1.2	330	21.8	119	8.1	68	21
97	−597.7	222	831	582	113	1.9	236	20.3	121	9.4	102	22
98	−600.3	269	492	158	115	1.7	304	24.2	136	10.4	85	26
100	−606.3	246	301	137	102	3.4	321	24.7	140	9.7	61	28
101	−622.3	241	432	158	92	2.9	308	21.5	121	8.6	50	23
102	−625.5	229	416	154	93	3.9	310	23.0	129	9.2	77	26

analyses are within error of the atmospheric ratio (Table 3), indicating no excess Ar. The plateau ages range from 2.83 ± 0.16 to 2.90 ± 0.22 Ma (Table 3). The different age determinations (plateau, normal isochron, and inverse isochron ages) of these samples all overlap within analytical error, providing independent confirmation of the reliability of these ages for the KSDP section. Units 37 and 75 are weakly altered and contained excess Ar, as evidenced by their U-shaped age spectra produced by step heating and their high initial $^{40}Ar/^{36}Ar$ values of 336 ± 3 and 342 ± 3, respectively. As a result, these samples did not produce valid ages.

The new KSDP ages are significantly older than those previously determined for Ko'olau lavas by K–Ar methods (2.9 vs. < 2.6 Ma). The KSDP ages indicate eruption in the Gauss normal magnetic period, which is consistent with a paleomagnetic study of the core (Herrero-Bervera et al. 2002). These new ages indicate that subaerially erupted Ko'olau shield-stage lavas overlap in age with Wai'anae post-shield lavas (2.90–3.06 Ma; Presley et al. 1997). This is the first definitive evidence that the Ko'olau and Wai'anae volcanoes erupted simultaneously.

Ko'olau geochemistry

Previous studies of Ko'olau basalts (Wentworth and Winchell 1947; Stille et al. 1983; Roden et al. 1984; Budahn and Schmitt 1985; Frey et al. 1994; Roden et al. 1994; Eiler et al. 1996; Hauri 1996; Lassiter and Hauri 1998) demonstrated that these lavas represent a geochemical and isotopic end member among Hawaiian shield tholeiites. Ko'olau lavas have the highest observed SiO_2, Al_2O_3 and Na_2O, and the lowest observed Fe_2O_3 and CaO at a given MgO, leading to their correspondingly high Al_2O_3/CaO and Na_2O/CaO among Hawaiian tholeiitic basalts (Frey et al. 1994). The high Sr, La, Zr, and relatively low Nb concentrations in Ko'olau surface lavas create high Zr/Nb, Sr/Nb, and La/Nb (Frey et al. 1994).

Subaerial weathering in Hawaii's tropical environment can significantly alter the composition of basalts. For example, surface alteration decreases K_2O, SiO_2, and CaO and increases Fe_2O_3, Al_2O_3, and TiO_2 in shield lavas (e.g., Feigenson et al. 1983; Lipman et al. 1990; Frey et al. 1994). In order to gain a more reliable understanding of KSDP lavas with respect to previous studies of Ko'olau and other Hawaiian shields, the effects of alteration were evaluated.

Most KSDP rotary-drilled samples (72%) have low K_2O/P_2O_5 values (< 1.2) compared to magmatic values of 1.5–2.0 (Wright and Fiske 1971). Some of these lavas also have significant loss on ignition (LOI) values > 0.6 wt% (Table 4). In contrast, most of the KSDP core (74%) and Wa'ahila Ridge samples (67%) are relatively unaltered (Table 4), consistent with petrographic observations (Table 2, Fig. 3).

The effects of alteration on the distinctive major element signatures of Ko'olau lavas (e.g., high Al_2O_3/CaO and Na_2O/CaO values) appear to be minor if we assume K_2O/P_2O_5 is a good indicator of alteration (e.g., Frey et al. 1994). The Al_2O_3 contents of these samples are relatively high at a given MgO, perhaps as a result of removal of other oxides through weathering (Table 4). Surface Ko'olau lavas from Makapu'u Head and the

WAFB core do not show significant changes in Al_2O_3/CaO with decreasing K_2O/P_2O_5, except two strongly fractionated lavas that may have undergone cpx fractionation (Fig. 4). All altered samples from Wa'ahila Ridge and the KSDP (save the most highly altered flow, unit 88, with the highest LOI) fall within the geochemical range of Al_2O_3/CaO values of unaltered KSDP flows (Fig. 4). Post-magmatic alteration did not significantly modify Al_2O_3/CaO values in the vast majority of Ko'olau lavas, although only the freshest portions of these flows were analyzed.

Ko'olau Na_2O/CaO is unmodified by alteration; all samples with $K_2O/P_2O_5 < 1.2$ have Na_2O/CaO values within the range of unaltered Ko'olau rocks, regardless of their extent of alteration. Similar results have been found by M. Vollinger (2002, personal communication) for Al_2O_3/CaO and Na_2O/CaO in Mauna Loa lavas. Nonetheless, only those samples with $K_2O/P_2O_5 \geq 1.2$ from the H3 tunnel (68% of published analyses) and Makapu'u (65% of published analyses) are included in the diagrams for comparison. However, the altered KSDP rotary samples are included in subsequent geochemical diagrams because so few were unaltered; they are identified with smaller symbols on the figures (e.g., Fig. 5).

KSDP whole-rock major element composition

A wide range in MgO content is shown by KSDP lavas (6.6–21.7 wt%; Table 4), typical of tholeiites from Hawaiian volcanoes (Frey et al. 1991; Clague et al. 1995). Above 7.5 wt% MgO, major element oxides define broad linear trends vs. MgO (Fig. 5). These features are indicative of olivine-controlled crystal fractionation and accumulation (e.g., Wright and Fiske 1971). The range of SiO_2 content in KSDP rocks is remarkably large at a given MgO (up to 3 wt%) compared to typical Hawaiian shield lavas (~1 wt% at Kīlauea; Quane et al. 2000). However, KSDP samples also have relatively high SiO_2 compared to tholeiites from some Hawaiian volcanoes (e.g., Kīlauea and Mauna Kea; Frey et al. 1994; Rhodes 1996).

The major element compositions of KSDP and Wa'ahila Ridge lavas are intermediate between typical surface Ko'olau compositions and those of the Mauna Loa volcano (Fig. 5). Most KSDP and Wa'ahila Ridge samples have generally lower Na_2O and higher CaO at a given MgO than typical Ko'olau lavas and many plot within the Mauna Loa field (Fig. 5). Compositions of H3 tunnel samples overlap with KSDP data, but most have low MgO abundances and plot where the Ko'olau and Mauna Loa fields overlap (Fig. 5).

Plots of Al_2O_3/CaO and Na_2O/CaO vs. MgO illustrate the compositional differences between KSDP and surface Ko'olau rocks (Fig. 5). Typical Ko'olau lavas have Al_2O_3/CaO > 1.45 (aver. = 1.51) and Na_2O/CaO > 0.26 (aver. = 0.30), although several Makapu'u lavas have lower Al_2O_3/CaO due to significant

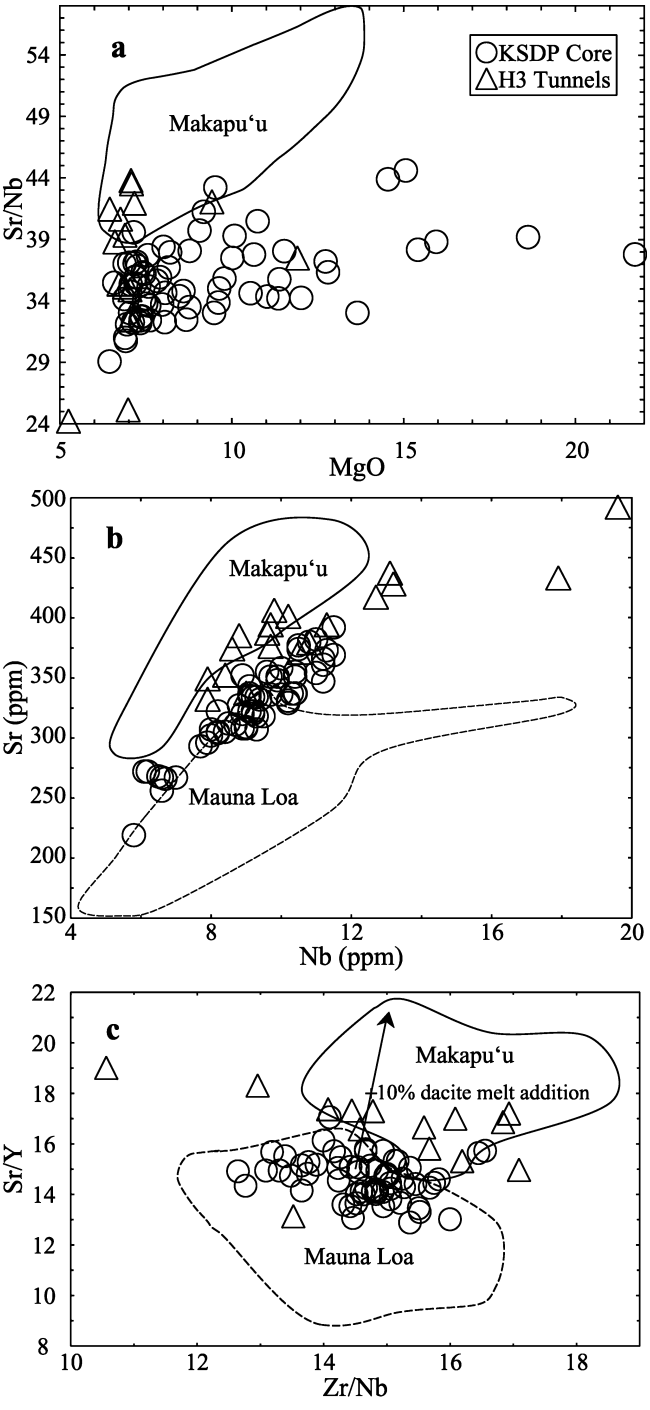

Fig. 6a–c Whole-rock trace element diagrams for KSDP and H3 tunnel lavas. **a** Sr/Nb vs. MgO. The lack of correlation on this plot and the scarcity (< 2 vol%) of plagioclase phenocrysts in most KSDP lavas (Table 2) indicate that plagioclase crystallization has not significantly modified the Sr/Nb ratio in these lavas, except in highly fractionated H3 lavas. **b** Sr vs. Nb plot shows that KSDP lavas are intermediate between typical Makapu'u and Mauna Loa lavas. **c** Sr/Y vs. Zr/Nb. Most KSDP samples plot within the Mauna Loa field; H3 samples are mostly in the Makapu'u field. The *arrow* indicates the effect of adding dacitic melt from eclogite (Sr/Y = 90; Norman and Garcia 1999) to an average KSDP lava composition. H3 data are from Jackson et al. (1999)

Table 6 Microprobe analyses of major elements in KSDP glasses

Unit	Elev. (m)	#[a]	SiO_2	TiO_2	Al_2O_3	FeO*[b]	MnO	MgO	CaO	Na_2O	K_2O	P_2O_5	Total
7	−324.3	4	52.82	2.32	14.42	10.21	0.12	6.40	10.65	2.22	0.44	0.22	99.61
8	−326.6	28	52.47	2.23	14.18	9.99	0.17	6.91	10.57	2.41	0.41	0.21	99.33
17	−353.3	18	52.33	2.61	13.77	11.18	0.22	6.28	10.53	2.62	0.34	0.27	99.87
22	−366.2	25	52.80	2.20	14.27	10.31	0.17	6.52	10.31	2.53	0.40	0.20	99.50
26	−373.9	9	53.28	2.64	13.71	11.29	0.17	5.85	10.09	2.33	0.28	0.24	99.65
27	−377.1	4	52.96	2.49	13.78	10.95	0.16	6.25	10.59	2.40	0.38	0.24	99.95
29	−381.1	5	52.31	2.51	13.88	10.91	0.16	6.30	10.36	2.09	0.47	0.25	99.26
33	−389.9	7	51.36	2.34	14.25	10.59	0.15	7.11	10.88	2.13	0.40	0.21	99.41
39	−402.7	6	50.97	2.81	13.66	11.80	0.16	6.06	10.74	2.37	0.44	0.25	99.27
42	−409.0	5	51.20	2.50	14.12	10.81	0.21	7.01	11.14	2.57	0.40	0.20	100.16
47	−419.3[c]	6	52.13	2.59	13.88	11.19	0.17	6.41	10.64	1.65	0.49	0.24	99.41
50	−432.4	4	52.39	2.39	14.26	10.09	0.11	6.46	10.62	2.37	0.50	0.23	99.42
55	−445.5	4	51.66	2.72	13.74	11.15	0.14	6.25	10.62	2.27	0.50	0.25	99.30
56	−446.3	4	51.52	2.75	13.83	11.51	0.12	6.07	10.38	2.29	0.54	0.29	99.29
57	−449.8	4	51.96	2.91	13.40	11.16	0.24	6.22	10.32	2.62	0.72	0.25	99.80
60	−459.9	4	52.21	3.21	13.05	12.25	0.20	5.27	9.75	2.57	0.60	0.28	99.38
63	−480.6	5	51.82	2.90	13.47	11.81	0.18	5.74	10.01	2.22	0.55	0.27	98.97
67	−512.6	5	52.99	2.28	13.98	10.50	0.16	6.17	10.13	2.18	0.40	0.24	99.03
74	−539.4	7	52.16	2.32	13.98	10.67	0.16	6.33	10.51	2.34	0.44	0.25	99.16
94	−588.3[c]	9	52.46	2.37	14.27	10.44	0.16	6.88	10.83	1.44	0.38	0.20	99.42
101	−615.6	6	51.02	2.36	14.27	10.39	0.17	7.08	10.98	2.37	0.36	0.23	99.21

[a]#, number of spot analyses averaged
[b]All iron as FeO
[c]Samples with significant Na_2O loss

plagioclase fractionation with little to no clinopyroxene crystallization. Only one unaltered sample from the Makapu'u section (KOO22 with 6.9 wt% MgO; Frey et al. 1994) has Al_2O_3/CaO and Na_2O/CaO below the typical Ko'olau values mentioned above. KSDP lavas average 1.34 and 0.23 for Al_2O_3/CaO and Na_2O/CaO, respectively. The few upper KSDP samples that have surface Ko'olau compositions (Al_2O_3/CaO $>$ 1.45 and Na_2O/CaO $>$ 0.26) will be discussed below. Typical Mauna Loa lavas have distinctly lower Al_2O_3/CaO and Na_2O/CaO ratios of ~1.28 and ~0.21, respectively (Fig. 5). Only low-MgO ($<$ 5.8 wt%) Mauna Loa lavas fractionated sufficient clinopyroxene and/or plagioclase to reach Na_2O/CaO values $>$ 0.26, the range typical of Makapu'u lavas.

KSDP whole-rock trace element compositions

Trace element abundances in cored KSDP lavas range widely but show systematic behavior (Table 5, Fig. 6). Ni and Cr abundances are positively correlated with MgO, consistent with the presence of olivine and spinel in these lavas. Sr and Nb abundances are positively correlated, as observed in previous Ko'olau studies (Frey et al. 1994), but KSDP lavas have lower Sr at a given Nb (Fig. 6b). This is reflected in the plot of Sr/Nb vs. MgO, which demonstrates that the low Sr is not related to plagioclase fractionation, which occurs in lavas with MgO $<$ 7 wt% (Fig. 6a). The KSDP Sr vs. Nb trend is intermediate between Ko'olau and Mauna Loa lavas, a distinctive trace element feature of KSDP core lavas (other similarly incompatible elements such as Ce and Zr also have intermediate abundances, but overlap with the surface Makapu'u and Mauna Loa data). Moderately incompatible elements in H3 lavas overlap the Makapu'u and KSDP fields (Fig. 6).

KSDP glass major element compositions

Volcanic glass is common at flow and intraflow contacts within the KSDP core. A majority of these 65 glasses (~55%) have an altered appearance (waxy, dull luster and reddish color from oxidation, or are strongly opaque) and were not analyzed. Ten of the analyzed glasses have heterogeneous compositions, based on multiple microprobe spot analyses, and/or low totals ($<$98.5 wt%), suggesting they are altered. Nineteen samples yielded uniform major element abundances, acceptable totals (98.5–100.2 wt%), and K_2O/P_2O_5 $>$ 1.5, suggesting that they are unaltered. However, two of these samples have low Na_2O ($<$2 wt%; Table 6), a feature shared with some subaerial Ko'olau flow and dike glasses (Garcia, unpublished data). They are more opaque than higher-Na_2O glasses and lack translucent brown edges. Palagonitization studies of basaltic glass have shown that significant loss of Na_2O and other oxides can occur even during low-temperature weathering (Jakobsson 1972; Furnes 1975).

The 17 unaltered KSDP glasses have a limited MgO range (5.3–7.1 wt%; Table 6). The highest SiO_2 content of a KSDP glass is 53.3 wt%, with a wide range (up to 2 wt%) at a given MgO. CaO and Al_2O_3 contents decrease with decreasing MgO (Figs. 7 and 8), indicating the importance of both clinopyroxene and

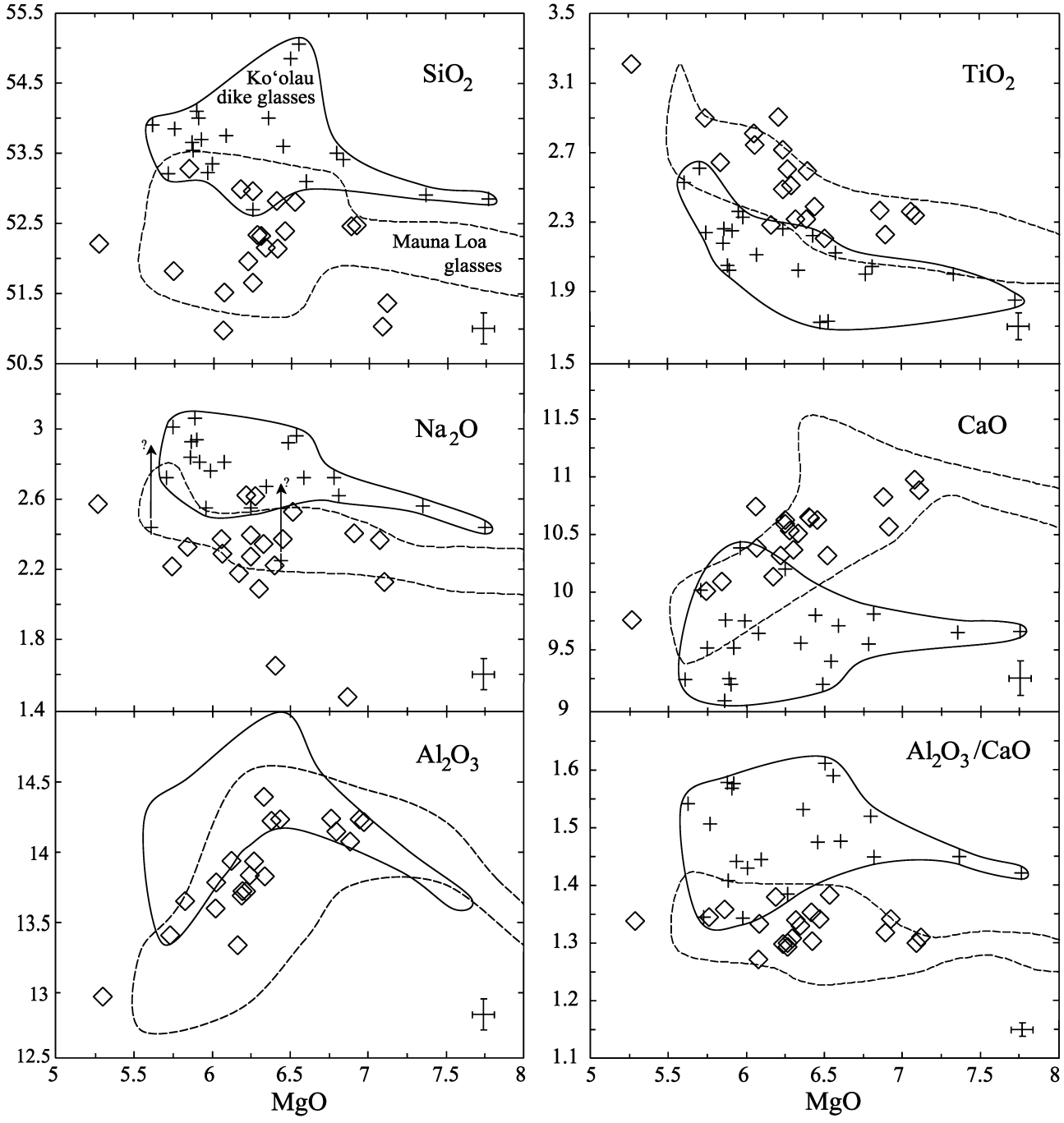

Fig. 7 MgO variation diagrams for KSDP glasses compared to those from Ko'olau dikes (*solid field*, *crosses*) and Mauna Loa (*dashed field*). These dikes cut and have similar major element compositions to Makapu'u-stage lavas. *Arrows* with *?* indicate two Ko'olau dike glasses that may have lost Na_2O (see text for discussion). Error bars in *lower right corner* represent two-sigma analytical error. Dike compositions are from Garcia (unpublished data)

plagioclase in the crystallization history of these glasses. This feature is consistent with the presence of both phases in KSDP lavas (Table 2). Compared to a suite of glasses analyzed in the same laboratory (Garcia, unpublished data) from dikes that cut and have compositions identical to surface Ko'olau lavas, KSDP glasses generally have higher CaO and TiO_2 as well as lower SiO_2 and Na_2O (Fig. 7). Like the whole-rock data, KSDP major element glass compositions are more similar to Mauna Loa glass, particularly for TiO_2 and SiO_2 vs. MgO trends (Fig. 7).

KSDP glass trace element compositions

A wide range of trace element abundances were determined on KSDP glasses by laser ablation ICP-MS (Table 7). These include all of the elements determined

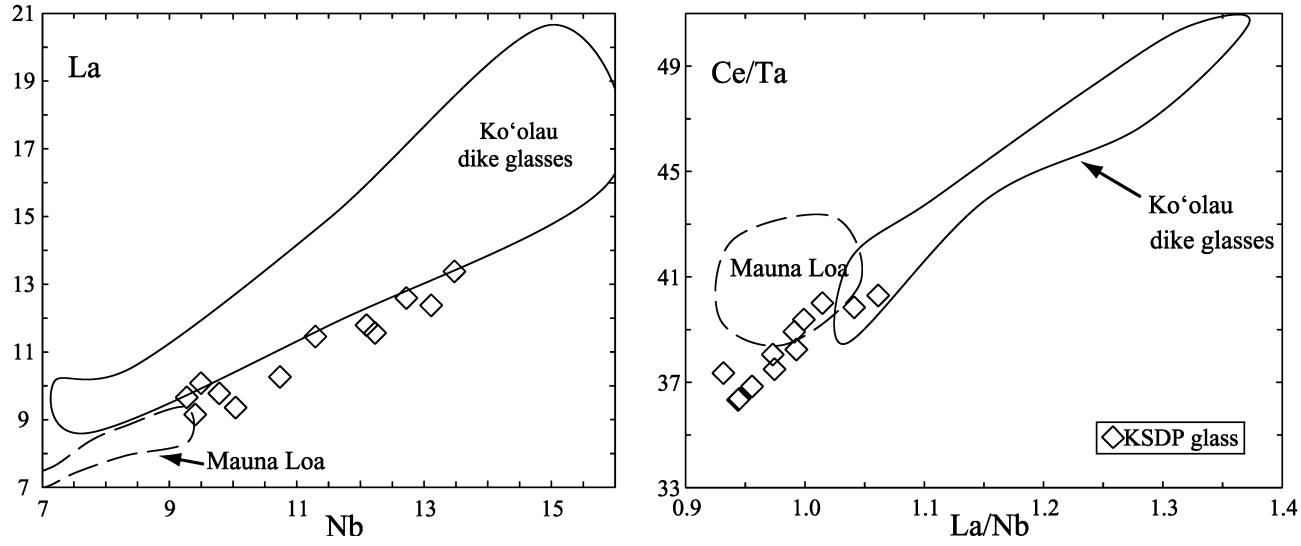

Fig. 8 Plots of ICP-MS data for strongly incompatible trace elements (Nb, Ta, La, and Ce) in KSDP glasses compared to surface Ko'olau dikes (Garcia et al., unpublished data data; *field* defined by 10 samples) and submarine Mauna Loa (Garcia et al. 1995; *field* defined by 12 samples). Note that KSDP glasses have higher incompatible abundances than those of Mauna Loa but lie on the same trend. HFSE abundances (Nb) are relatively low at given La values in Ko'olau dike glasses, and the corresponding ratios of Ce and La over Ta and Nb are high in these glasses. These ratios overlap for KSDP, Ko'olau dike glass and Mauna Loa glasses. The Ko'olau glasses are collinear on the ratio plot, although the dikes extend to much higher values. This trend suggests they share common source components

by XRF except Zn, and many others (e.g., REEs). The KSDP glasses show coherent variations for highly incompatible elements (Fig. 8). These variations are offset from typical Ko'olau dike glass compositions, but lie along the trend for Mauna Loa glasses (Fig. 8). For example, abundances of Nb are higher at a given La content than in Ko'olau dike glasses (Fig. 8). As a result, KSDP glasses have lower Ce/Ta and La/Nb values than Ko'olau dike glasses analyzed in the same laboratory. Additionally, the range of abundances of these trace elements is less than that of Ko'olau dike glasses, although both data suites have undergone similar amounts of fractionation (MgO ranges of ~2 wt%).

The compositional distinctions between KSDP and Ko'olau dike glass trace element abundances are also evident on plots normalized to primitive mantle (Sun and McDonough 1989) and the average Ko'olau dike glass composition (Fig. 9, Table 7). Most KSDP glasses have higher average abundances of middle to heavy REEs relative to Ko'olau dike glasses, as well as higher Ta, Nb, and U, and lower average abundances of the moderately incompatible elements (Sr, Pb, Pr, Ce, La) and the most highly incompatible elements (Ba, Rb, Cs). All KSDP glasses have positive Ta anomalies (Fig. 9a), while all but one Ko'olau dike glass samples have positive La anomalies and lower primitive mantle-normalized Ta than La values, suggesting the sources for these lavas may be distinct.

Discussion

Geochemical stratigraphy of the Ko'olau volcano

The results for KSDP lavas indicate that the subaerial shield stage of the Ko'olau volcano contains at least two geochemically distinct stages (Fig. 10). The upper stage is made up of petrographically and geochemically distinct Ko'olau flows that resemble those from the Makapu'u Head area (Frey et al. 1994). Henceforth, they are referred to as Makapu'u-stage lavas. Deeper KSDP lavas are petrographically and geochemically similar to those of Mauna Loa (Fig. 5), and are here called Kalihi-stage lavas for the KSDP location. The nature of the transition between the geochemically distinct stages of Ko'olau shield volcanism could not be clearly resolved in the rotary-drilled section of the KSDP or Wa'ahila Ridge holes because of the lack of recovery from 89 to 173 m b.s.l. for KSDP, poor sampling capabilities, and the alteration of most rock cuttings.

The lower sections from the KSDP and Wa'ahila Ridge holes have Mauna Loa-like Al_2O_3/CaO values (Fig. 10) and many contain cpx crystals with no opx (Table 2 and eTable 2). In contrast, the lavas from the upper sections of both holes have Makapu'u petrography and geochemistry. Unfortunately, most of the near-surface Wa'ahila lavas (to 136 m b.s.l.) were not suitable for chemical analysis (only one sample was unaltered). The three analyzed samples straddle the boundary between Makapu'u and Kalihi stages (Fig. 10). However, the petrography of these samples (82% contain opx and only 9% have cpx; eTable 2), are characteristic of Makapu'u-stage lavas.

In reexamining the chemistry of H3 tunnel lavas reported by Jackson et al. (1999), we found Al_2O_3/CaO values indicative of both the Kalihi and Makapu'u stages of shield development. Thus, the H3 section, with its more frequent and better sampling than the rotary-drilled sections of the KSDP and Wa'ahila wells,

Table 7 Laser ablation ICP-MS analyses of trace element abundances (ppm) in KSDP glasses. *Kdg* Average of 14 Ko'olau dike glasses (Makapu'u stage)

Unit	Cs	Rb	Ba	Th	U	Nb	Ta	La	Ce	Pr	Pb	Sr	Nd	Sm	Zr	Hf	Eu	Gd	Dy	Y	Ho	Er	Yb	Lu	V	Sc	Cr	Ni
7	0.057	6.23	86.1	0.63	0.19	9.50	0.63	10.1	25.4	3.74	1.09	337	18.9	5.21	144	3.56	1.84	5.53	5.24	24.6	1.00	2.46	2.02	0.29	256	30.3	220	85
8	0.060	5.81	77.5	0.62	0.19	9.27	0.61	9.66	24.4	3.51	1.08	347	18.0	5.04	137	3.46	1.76	5.39	4.84	23.4	0.94	2.26	1.95	0.27	255	29.9	300	106
17	0.075	7.18	92.6	0.77	0.25	12.1	0.79	11.8	29.7	4.23	1.22	358	21.4	5.93	159	4.07	2.02	6.31	5.64	26.8	1.07	2.64	2.24	0.32	282	31.4	167	63
22	0.061	5.93	78.6	0.63	0.21	9.78	0.63	9.78	24.7	3.51	0.99	344	17.8	5.04	136	3.39	1.78	5.45	4.83	23.5	0.93	2.28	1.91	0.27	244	29.5	282	71
27	0.066	6.35	90.0	0.76	0.23	11.3	0.73	11.5	29.0	4.16	1.23	355	21.1	5.78	159	3.99	1.98	6.14	5.46	26.3	1.04	2.59	2.18	0.31	270	30.9	165	63
42	0.057	6.03	75.0	0.67	0.21	10.7	0.71	10.3	26.3	3.78	1.05	338	19.6	5.61	149	3.81	1.93	6.07	5.57	27.0	1.08	2.66	2.26	0.32	277	33.4	229	72
50	0.080	7.29	94.4	0.79	0.24	12.2	0.79	11.6	28.7	4.06	1.15	330	20.1	5.53	151	3.78	1.87	5.58	4.98	23.9	0.96	2.29	1.97	0.28	249	27.6	122	55
55	0.078	7.76	97.9	0.82	0.27	12.7	0.81	12.6	31.6	4.52	1.30	387	22.7	6.14	171	4.28	2.16	6.51	5.69	27.7	1.10	2.68	2.27	0.32	298	33.6	198	70
57	0.075	7.21	88.2	0.81	0.27	13.1	0.86	12.4	31.4	4.50	1.22	377	22.9	6.44	179	4.41	2.20	6.71	6.07	29.7	1.19	2.86	2.39	0.34	305	33.6	161	61
63	0.077	8.27	104	0.86	0.28	13.5	0.87	13.4	33.4	4.74	1.41	405	23.7	6.50	181	4.42	2.26	6.83	6.09	29.4	1.16	2.82	2.35	0.33	315	35.0	174	71
67	0.058	5.01	67.8	0.62	0.20	10.0	0.64	9.35	24.1	3.48	0.97	321	17.8	4.95	136	3.41	1.70	5.28	4.79	23.1	0.93	2.24	1.85	0.27	248	29.5	291	77
101	0.057	5.07	67.9	0.58	0.19	9.41	0.62	9.15	23.5	3.41	1.11	336	17.6	5.03	134	3.46	1.80	5.48	4.96	24.1	0.97	2.38	2.04	0.29	264	31.2	245	88
Kdg	0.074	8.27	103	0.75	0.21	10.5	0.67	12.4	30.1	4.15	1.33	402	20.2	5.35	145	3.61	1.82	5.45	4.76	23.1	0.92	2.25	1.88	0.27	251	27.8	235	99

provides greater resolution of the geochemically transitional interval. The seven deepest analyzed lavas from the lowest 50 m of the H3 section all have Kalihi-stage Al_2O_3/CaO values. However, the nature of this transition is unresolved because only 19 of the 126 flows in this ~200 m thick section were analyzed, and only 13 of these 19 flows have $K_2O/P_2O_5 > 1.2$ (shown to scale in Fig. 10).

Glass analyses from the KSDP core and subaerial Ko'olau dike exposures also indicate a change in geochemistry (Figs. 7 and 8). All 19 unaltered KSDP core glasses have Kalihi-stage compositions (Fig. 10) and they extend to deeper depths than the unaltered whole-rock data (616 vs. 550 m b.s.l.; Fig. 10). Thus, the geochemically distinct Kalihi stage of the Ko'olau volcano persists for at least 400 m beneath Kalihi Valley.

Nature, duration and volume of Ko'olau intrashield stages

The original thickness of Ko'olau lava flows overlying the H3 section was estimated to be 500–600 m (Jackson et al. 1999). This is about twice our estimate of the thickness of Makapu'u-stage flows at the KSDP (at least 250 m, allowing for 150 m of erosion) and Wa'ahila sites (at least 175 m, allowing for 10 m of erosion). These differences are not surprising because of the known, rapid lava accumulation rate at near-summit locations, where the H3 section formed, compared to the flank locations for KSDP and Wa'ahila wells. For example, lava accumulation rates for the summit of an average Hawaiian shield are estimated at 13–23 mm/year (DePaolo and Stolper 1996) compared to lower estimates for the coastal flanks of Mauna Kea (7.8 ± 3.2 mm/year; Sharp et al. 1996) and Mauna Loa (0.9 mm/year; Lipman 1995). These accumulation rate approximations are used below to make broad estimates concerning the geochemically distinct Makapu'u stage of the Ko'olau volcano.

The distinct Makapu'u-stage compositions cover virtually the entire subaerial surface of the Ko'olau volcano (Frey et al. 1994). For example, all 35 flows within the 200-m cored interval at the WAFB and all Makapu'u flows sampled over a 250-m composite section have Makapu'u-stage compositions. No soils or other obvious indicators of a hiatus or reduction in lava eruption rates were observed in any of the studied sections. Thus, if we assume no change in lava accumulation rate within the Makapu'u stage and apply the 13–23 mm/year rate of DePaolo and Stolper (1996) to the near-summit H3 section, it could have been formed over a period of 22–46 ka. Multiplying this eruptive duration range by the only well-known value for the average eruption rate of the shield stage of a Hawaiian volcano (0.05 km^3/year for historical Kīlauea; Dvorak and Dzurisin 1993) gives a 1,100–2,300 km^3 volume for the Makapu'u stage. The lower margin of this estimate is consistent with a recent, independent estimate for

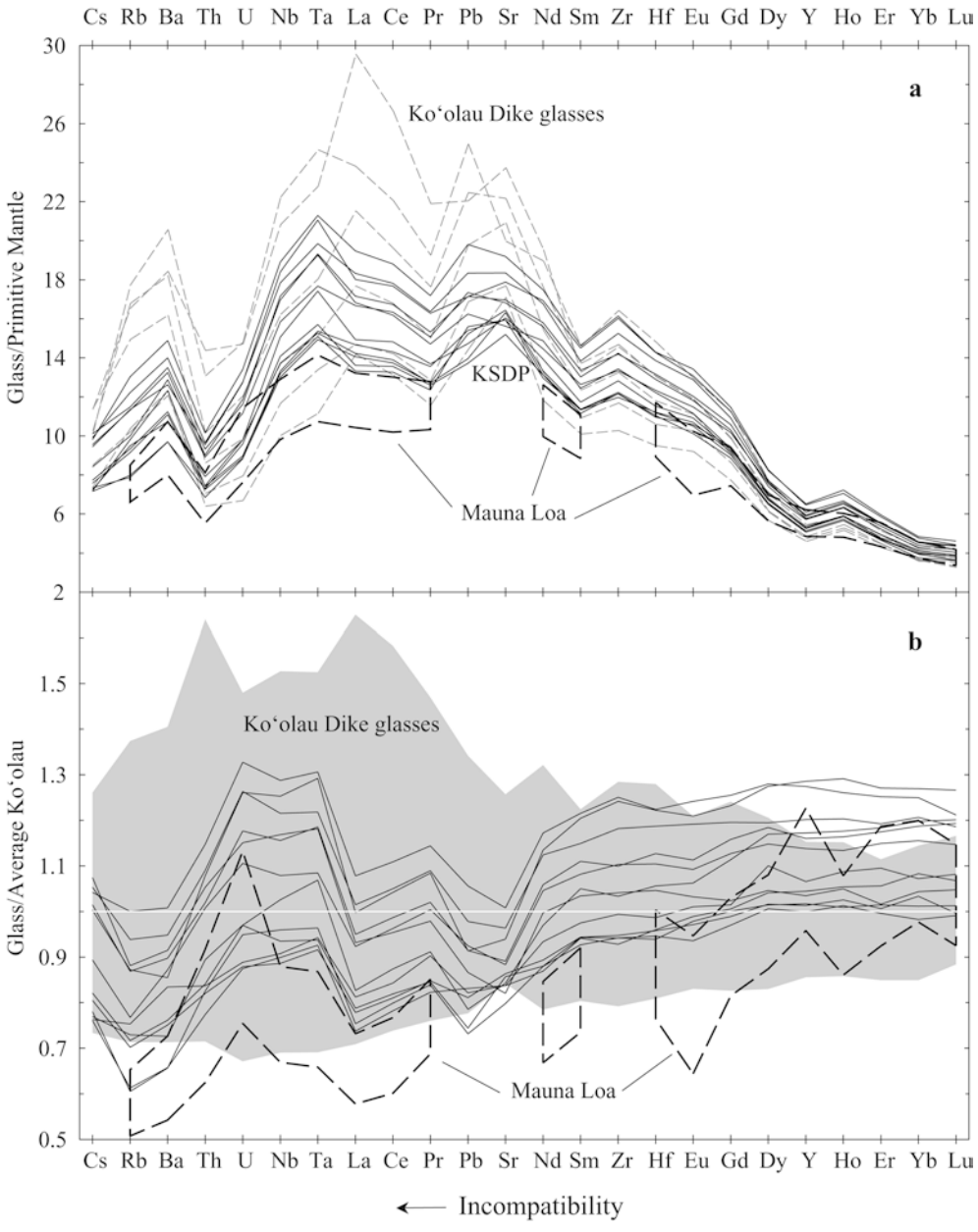

Fig. 9a, b Trace element variation diagrams for KSDP glasses. **a** Primitive mantle plot using normalizing values from Sun and McDonough (1989). **b** Plot of values normalized to an average Ko'olau dike glass composition (10 samples from Garcia, unpublished data, *shaded fields*; see Table 7). Mauna Loa ICP-MS analyses (Garcia et al. 1995) are included for comparison. Note the wide range of Ko'olau dike glass compositions and their relative enrichment of LREEs to HREEs, as well as the high Nb and Ta abundances in KSDP lavas relative to La and Ce. A linear scale has been used for the y-axis, rather than the traditional log scale, to highlight differences among the glasses. All analyses were determined in the same laboratory to avoid interlaboratory bias

these geochemically distinct lavas (~1,000 km^3; Takahashi and Nakajima 2002).

Recycled oceanic crust in the Hawaiian source?

A debate has arisen on the nature of the source component that creates the distinctive chemistry of Ko'olau lavas. It has long been argued that variable degrees of melting of peridotitic mantle cannot produce the major and trace element compositions and isotopic signatures of all Hawaiian lavas (Hofmann and White 1982). In particular, the high SiO_2, positive Sr anomalies in olivine-hosted melt inclusions, and distinctive Os isotopic data were used to indicate that subducted oceanic crust, metamorphosed to eclogite, is a significant source component for at least some Hawaiian magmas, especially those from Ko'olau (e.g., Hauri 1996; Lassiter and Hauri 1998). Two new experimental petrology studies examined the issue of whether recycled oceanic

►

Fig. 10 Whole-rock and glass Al_2O_3/CaO from KSDP and Wa'ahila Ridge samples vs. depth (relative to sea level). *Symbols* are as in previous figures or as noted. Mauna Loa whole-rock range from J.M. Rhodes (2002, personal communication), glass range from Garcia et al. (1989). All Mauna Loa lavas and glasses with < 5.8 wt% MgO are not included to reduce clinopyroxene and plagioclase fractionation effects on trends. Eight Makapu'u lavas containing significant plagioclase have low Al_2O_3/CaO (< 1.45) and were removed. The H3 tunnel section rocks, which straddle the transition between Kalihi and Makapu'u stages, are shown for comparison. Typical subaerial Ko'olau lavas do not significantly fractionate clinopyroxene. Moderately evolved Ko'olau dike glass compositions (< 6.5 wt% MgO) are dominated by plagioclase fractionation, leading to lower Al_2O_3/CaO values than whole-rock data

crust is the "exotic" component in Ko'olau magmas, and reached conflicting interpretations (Takahashi and Nakajima 2002; Pertermann and Hirschmann 2003). Here, we utilized the geochemistry of KSDP lavas and glasses to provide constraints for evaluating the source composition and melting processes for the Ko'olau

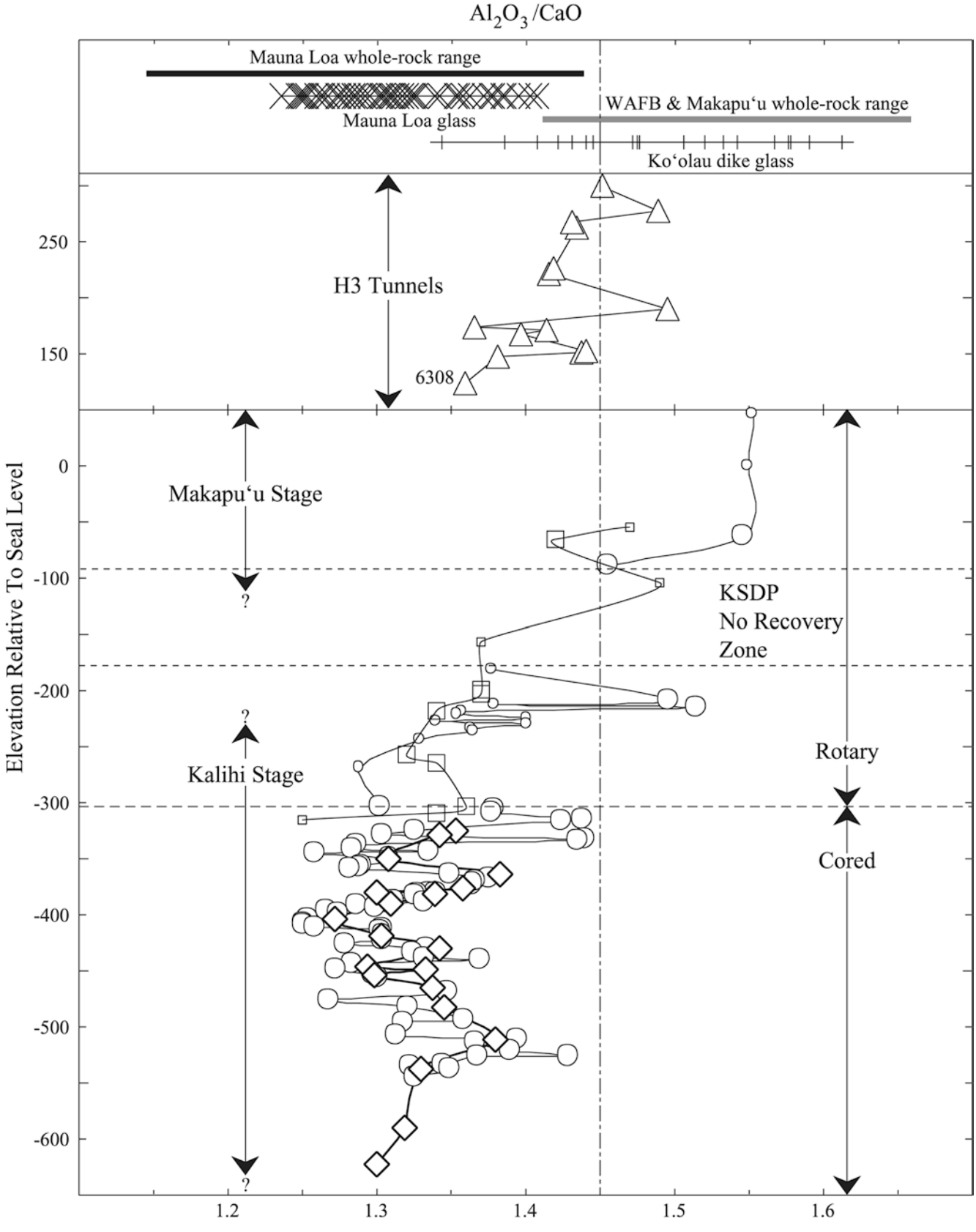

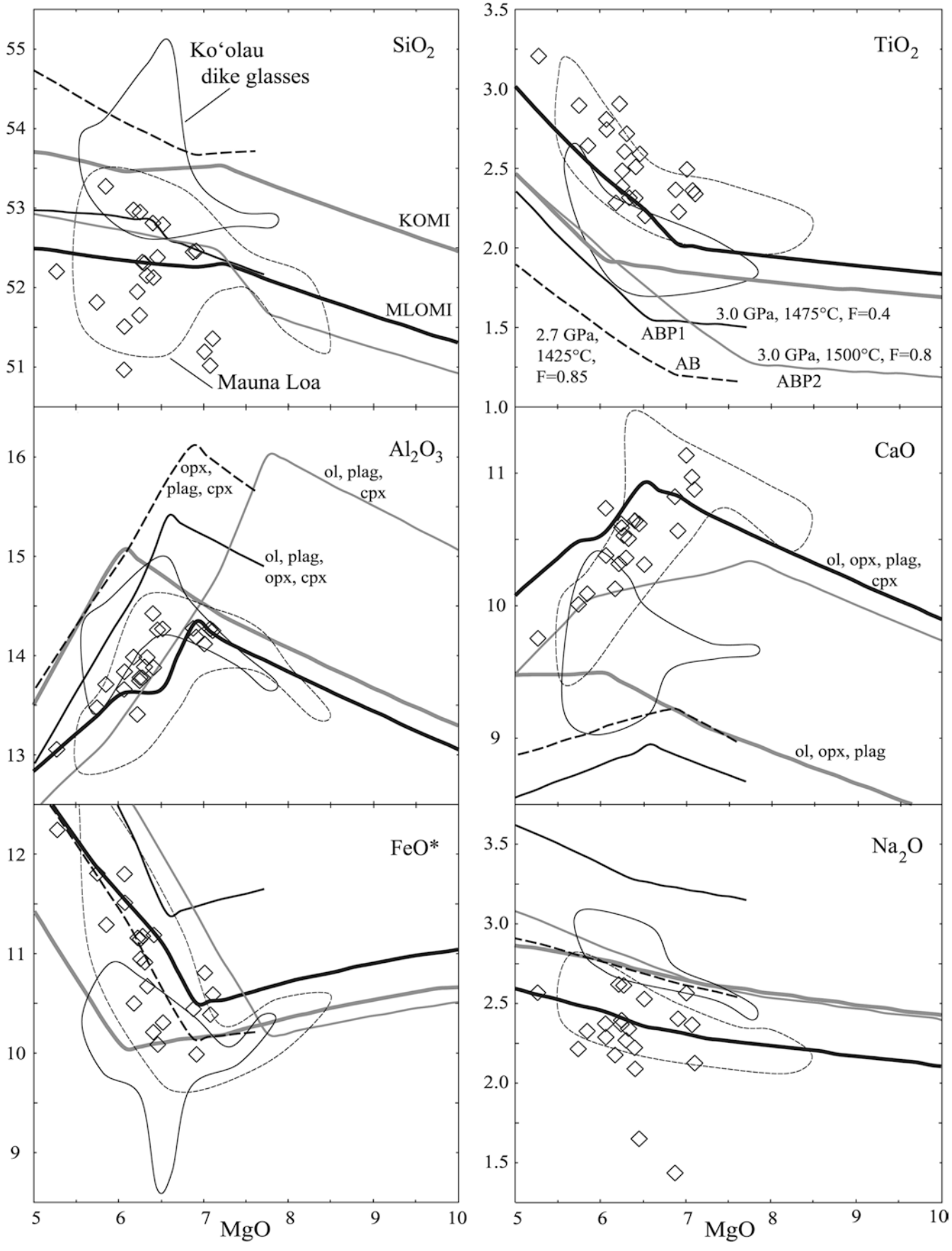
SiO2
Ko'olau
dike glasses
KOMI
MLOMI
Mauna Loa
TiO2
3.0 GPa, 1475°C, F=0.4
ABP1
2.7 GPa,
1425°C,
F=0.85
AB
3.0 GPa, 1500°C, F=0.8
ABP2
Al2O3
opx,
plag, cpx
ol, plag,
cpx
ol, plag,
opx, cpx
CaO
ol, opx, plag,
cpx
ol, opx, plag
FeO*
Na2O
MgO
MgO

◄

Fig. 11 Fractional crystallization paths for experimentally created, potential Ko'olau parental magmas from Takahashi and Nakajima (2002; *AB* Archean basalt, *ABP1* and *ABP2* peridotite + Archean basalt) and representative Ko'olau and Mauna Loa olivine-hosted melt inclusions (*KOMI* and *MLOMI*; Norman et al. 2002), compared to Kalihi- (*diamonds*) and Makapu'u-stage glass compositions and Mauna Loa glasses (*fields*). Experimental conditions, estimated degree of melting (*F*), and crystallization sequences are as labeled. Crystallization paths were determined using MELTS (Ghiorso and Sack 1995), under the conditions 0.5 kbar, QFM-1, and 0.1 wt% H_2O (see text for discussion)

volcano, and the processes that caused the distinctive change in the shield-stage geochemistry for this volcano.

One of the distinctive geochemical features of Makapu'u-stage lavas is their high Sr/Y values compared to other Hawaiian shield volcanoes (Norman and Garcia 1999; Fig. 6). Although lower degrees or lower pressures of melting can explain the differences in major elements for Kalihi- vs. Makapu'u-stage flows, the high Sr/Y (Fig. 6), lower high field strength elements (e.g., Ta, Nb, Ti) and distinct Hf, Pb, Sr, and Os isotope ratios (Roden et al. 1994; Lassiter and Hauri 1998; Blichert-Toft et al. 1999) in the Makapu'u-stage lavas require another source component, such as garnet-bearing recycled oceanic crustal material.

High-pressure (2.7–3.0 GPa) melting experiments involving basalt, and mixtures of peridotite and basalt were undertaken to evaluate the potential of recycled oceanic crust for producing Ko'olau parental melt compositions (Takahashi and Nakajima 2002). To test whether these experiments were successful, we modeled liquid compositions created from melting Archean basalt (thought to more closely resemble the composition of ancient subducted oceanic lithosphere than modern MORB), and from sandwiches of mantle peridotite KLB-1 (Takahashi 1986) with Archean basalt (Takahashi and Nakajima 2002), using the thermodynamically based and experimentally calibrated MELTS program (Ghiorso and Sack 1995). Our modeling goal was to evaluate whether the "primary" liquids from the experimental studies lie along crystal fractionation paths defined by KSDP or Ko'olau glass data. For comparison, we also modeled the evolution of the average of 111 typical Ko'olau melt inclusions from two picritic basalts and 160 inclusions from three Mauna Loa picrites (Norman et al. 2002). The MELTS calculations were made using low pressures (0.1 GPa) indicative of the shallow (2–3 km) Hawaiian shield summit magma chambers (Decker et al. 1983; Klein et al. 1987), relatively dry water contents (0.1–0.4 wt%, based on water contents of Mauna Loa and Ko'olau glasses and inclusions; Hauri 2002; Davis et al. 2003), and relatively reduced oxygen fugacities (QFM to QFM-1; based on measured Fe^{2+}/Fe^{3+} in Hawaiian tholeiitic lavas; e.g., Byers et al. 1985).

None of the experimentally derived melt magma compositions of Takahashi and Nakajima (2002) match Makapu'u- or Kalihi-stage glass compositions (Fig. 11). In particular, model Al_2O_3 crystal fractionation paths are too high to match any Ko'olau tholeiite. In contrast, the higher MgO (11.7 wt%) average Mauna Loa melt inclusion compositions from Makapu'u picrites yielded liquid lines of descent similar to Makapu'u-stage glass compositions but distinct from the Kalihi-stage compositions (Fig. 11). Not surprisingly, the average of Mauna Loa melt inclusion composition produced a liquid fractionation path that descends through the field of KSDP glasses (Fig. 11), which are compositionally similar to Mauna Loa. Likewise, a new experimental study of MORB-like eclogite by Pertermann and Hirschmann (2003) was unable to create any suitable parent liquid composition for Ko'olau magmas. Furthermore, they argued that no other experimental study has produced a suitable parental composition from melting eclogite. However, Pertermann and Hirschmann (2003) speculated that mixing of peridotite melt (Kīlauea picrite KIL-1–7 from Norman and Garcia 1999) with 20–35% of a hypothetical basaltic andesitic melt might produce compositions like Ko'olau melt inclusions, although they were unable to produce such a melt with the appropriate composition.

Another complication in producing Ko'olau parental magma compositions is the evidence of other components in the source for Hawaiian magmas. For example, high-Sr melt inclusions in Mauna Loa olivines (Sobolev et al. 2000) and the high Sr abundances of all Ko'olau lavas (Fig. 6) might be attributed to the involvement of plagioclase-rich gabbroic cumulates from recycled oceanic crust. Also, a sediment source has been invoked to explain the distinctive Os, Pb and Hf isotopic data for Ko'olau lavas (Blichert-Toft et al. 1999). Neither of these components was considered in previous melting experiments. Thus, we conclude that Archean basalt was probably only one of many lithospheric components that were subducted, metamorphosed to high grade, entrained in the Hawaiian plume, partially melted, and mixed with mantle peridotite melts to form the parental magmas of the Ko'olau volcano.

Qualitatively, the compositional change from Kalihi- to Makapu'u-stage lavas, which occurred near the end of Ko'olau shield volcanism, might be explained by the addition of melt from recycled oceanic crust. An increase in the proportion of pyroxenite to peridotite-derived melts would be expected at the end of Ko'olau shield volcanism as the degree of source melting decreased with the drift of the volcano off the hotspot (Takahashi and Nakajima 2002). Norman and Garcia (1999) estimate a contribution of only ~10% melt from a pyroxenitic source would be needed to explain the trace element characteristics of Makapu'u-stage lavas. However, if an increase in the pyroxenitic component is a normal consequence of the death of Hawaiian shield volcanoes, why is this component only observed at Ko'olau?

One dramatic event that affected the Ko'olau volcano near the end of its shield volcanism was the catastrophic collapse of its northeast flank (Moore et al. 1994).

Approximately 40% of the volcano is thought to have broken away in a giant landslide (Satake et al. 2002). Such a massive unloading event has the potential to have affected the melting regime and caused a change in lava composition (e.g., Presley et al. 1997). However, a rapid decrease in confining pressure would be expected to produce a higher degree of melting, rather than the source change or decrease in degree of melting inferred from this study. Also, the change in lava composition occurred over a significant time interval, as indicated by the at least 60-m-thick sequence of transitional H3 tunnel lavas, rather than abruptly as might be expected following a giant landslide. Furthermore, rare lavas with Makapu'u-like mineralogies and compositions occur below this transition within the KSDP cored section (Fig. 10; Table 2). If volcanic activity stopped completely after Kalihi-stage lavas were erupted, the Nu'uanu landslide could have played a role in creating Makapu'u-stage lavas by reviving the volcano through unloading. However, there is no evidence for any gap in Ko'olau volcanism as would be indicated by a soil or erosional feature, and Makapu'u-stage lavas compose the subaerial portion of the Nu'uanu landslide scarp, indicating that they predate the landslide. Changes in lava composition have been observed near the end of shield volcanism at several Hawaiian volcanoes (e.g., Mauna Loa, Kurz et al. 1995; Kauai, Mukhopadhyay et al. 2003). Thus, as these volcanoes drift away from the hotspot, minor source components with lower melting temperature may play a larger role in magma genesis.

Conclusions

This study examined Ko'olau shield-stage lava rock cuttings from two rotary-drilled wells located in Kalihi Valley and on Wa'ahila Ridge. We deepened the Kalihi well by coring to a depth of 632 m b.s.l. This coring phase, termed the Ko'olau Scientific Drilling Project (KSDP), achieved ~95% recovery and revealed 103 subaerially erupted lava flows (67% pāhoehoe) and one sedimentary unit. The KSDP core, which was Ar–Ar dated at ~2.9 Ma, displays Mauna Loa-like major element compositions distinct from surface Ko'olau lavas. The geochemistry of these lavas reveals a source change and declining degree of melting. The characteristically high SiO_2, Al_2O_3/CaO, Na_2O/CaO, and large ion lithophile abundances of surface Ko'olau lavas are named here the Makapu'u stage. The transition between these compositional stages occurred over a brief but significant time period (2,600–4,600 years), indicating that the process that caused the change was more gradual than could be explained by a catastrophic unloading event such as the giant Nu'uanu landslide. The distinctive high SiO_2 and relatively low TiO_2, Nb, and Ta abundances of Ko'olau lavas may be explained by entrainment and lower degrees of melting of a lithologically diverse block of recycled oceanic crust in the Hawaiian plume. However, experimental studies of melts produced from mixtures of peridotite and materials thought to resemble recycled oceanic crust (Yaxley and Green 1998; Takahashi and Nakajima 2002, Pertermann and Hirschmann 2003) have been unsuccessful in producing suitable parental magma compositions. Perhaps other components such as plagioclase-rich gabbros and deep-sea sediments are required. As the volcano drifted away from the hotspot, recycled oceanic crust components became more involved in producing Ko'olau magmas.

Acknowledgements We owe a great debt to Honolulu Board of Water Supply chief geologist Chester Lao for providing rotary drill cuttings from the Kalihi and Wa'ahila Ridge holes, assistance in obtaining drilling permits, and permission to deepen the Kalihi water observation hole. Thanks also to the DOSECC team for providing expert coring services, particularly Dennis Nielson, Theresa Fall, engineer Bruce Howell and drillers Vance Hyatt and Kiki Kama. Mahalo nui loa to Dave Whilldin for his aid during drilling setup, and to core processing volunteers Mike Davis, Melissa Ito, Nate Adams, and Toby Vana. We are indebted to J.M. Rhodes and Eiichi Takahashi for providing datasets for comparison, and to Mike Vollinger and Marc Norman for their assistance in obtaining XRF and ICP-MS analyses, respectively. Dating of samples in the labs of Robert Duncan (Oregon State University) and Terry Spell (University of Nevada at Las Vegas), paleomagnetic work by Rebecca Carey, and emergency thin sections provided by JoAnn Sinton were of great benefit to this study. Microprobe analyses were supported by a University of Hawaii Harold T. Stearns foundation grant. E.H. is grateful for the insight received from John Sinton and Donald Thomas on his M.Sc. thesis, which this paper is based on. The reviews of Fred Frey and Greg Yaxley greatly improved this manuscript. This work was supported by a joint grant from the Earth Science and Ocean Science Divisions of the National Science Foundation (OCE 99-08911), and by generous matching funds from the University of Hawai'i, California Institute of Technology (E.M. Stolper), U.C. Berkeley (D. DePaolo), Massachusetts Institute of Technology (F. Frey), Carnegie Institute of Washington (E. Hauri), Max Plank Institut für Chemie (A. Hofmann), Woods Hole Oceanographic Institute (M. Kurz), and the Tokyo Institute of Technology (E. Takahashi). This is SOEST contribution #6319.

References

Achterbergh EV, Ryan CG, Jackson SE, Griffin WL (2001) Data reduction software for LA-ICP-MS. In: Sylvester PJ (ed) Laser ablation ICP-MS in the Earth Sciences. Mineral Assoc Can Short Course 29:239–243

Blichert-Toft J, Frey FA, Albarede F (1999) Hf isotope evidence for pelagic sediments in the source of Hawaiian basalts. Science 285:879–882

Budahn JR, Schmitt RA (1985) Petrogenetic modeling of Hawaiian tholeiitic basalts; a geochemical approach. Geochim Cosmochim Acta 49:67–87

Byers C, Garcia MO, Muenow D (1985) Volatiles in pillow rim glasses from Loihi and Kīlauea volcanoes, Hawaii. Geochim Cosmochim Acta 49:1887–1896

Cande SC, Kent DV (1995) Revised calibration of the geomagnetic polarity timescale for the Late Cretaceous and Cenozoic. J Geophys Res 100:6093–6095

Chappell BW (1991) Trace element analysis of rocks by X-ray spectrometry. In: Barrett CS, Gilfrich JV, Noyan IC, Huang TC, Predecki PK (eds) Proc 39th Annu Conf Applications of X-ray analysis. Adv X-Ray Analysis 34:263–276

Clague DA, Dalrymple GB (1987) The Hawaiian-Emperor volcanic chain. Part I. Geologic evolution. In: Decker RW, Wright TL, Stauffer PH (eds) Volcanism in Hawaii. US Geol Surv Prof Pap 1350:5–73

Clague DA, Moore JG, Dixon JE, Friesen WB (1995) Petrology of submarine lavas from Kīlauea's Puna Ridge, Hawaii. J Petrol 36:299–349

Davis MG, Garcia MO, Wallace P (2003) Volatiles in Mauna Loa glasses: implications for magma degassing and contamination, and growth of Hawaiian volcanoes. Contrib Mineral Petrol 144:570–591

Decker RW, Koyanagi RY, Dvorak JJ, Lockwood JP, Okamura AT, Yamashita KM, Tanigawa WR (1983) Seismicity and surface deformation of Mauna Loa Volcano, Hawaii. EOS Trans Am Geophys Union 64:545–547

DePaolo DJ, Stolper EM (1996) Models of Hawaiian volcano growth and plume structure; implications of results from the Hawaii Scientific Drilling Project. J Geophys Res 101:11,643–11,654

Doell RR, Dalrymple GB (1973) Potassium-argon ages and paleomagnetism of the Waianae and Koolau Volcanic Series, Oahu, Hawaii. Geol Soc Am Bull:1217–1241

Donaldson CH (1976) An experimental investigation of olivine morphology. Contrib Mineral Petrol 57:187–213

Dvorak JJ, Dzurisin D (1993) Variations in magma supply rate at Kīlauea Volcano, Hawaii. J Geophys Res 98:22,255–22,268

Eggins SM, Kinsley LPJ, Shelley JMG (1998) Deposition and element fractionations processes during atmospheric pressure laser sampling for analysis by ICP-MS. Appl Surface Sci 127/129:278–286

Eiler JM, Farley KA, Valley JW, Hofmann AW, Stolper EM (1996) Oxygen isotope constraints on the sources of Hawaiian volcanism. Earth Planet Sci Lett 144:453–468

Feigenson MD, Hofmann AW, Spera FJ (1983) Case studies on the origin of basalt. II. The transition from tholeiitic to alkalic volcanism on Kohala Volcano, Hawaii. Contrib Mineral Petrol 84:390–405

Frey FA, Garcia MO, Wise WS, Kennedy A, Gurriet P, Albarede F (1991) The evolution of Mauna Kea Volcano, Hawaii; petrogenesis of tholeiitic and alkalic basalts. J Geophys Res 96:14,347–14,375

Frey FA, Garcia MO, Roden MF (1994) Geochemical characteristics of Koolau Volcano; implications of intershield geochemical differences among Hawaiian volcanoes. Geochim Cosmochim Acta 58:1441–1462

Furnes H (1975) Experimental palagonization of basaltic glasses of varied composition. Contrib Mineral Petrol 50:105–113

Garcia MO, Muenow DW, Aggrey KE, O'Neil JR (1989) Major element, volatile, and stable isotope geochemistry of Hawaiian submarine tholeiitic glasses. J Geophys Res 94:10,525–10,538

Garcia MO, Hulsebosch T, Rhodes JM (1995) Olivine-rich submarine basalts from the southwest rift zone of Mauna Loa volcano: implications for magmatic processes and geochemical evolution. In: Rhodes JM, Lockwood JP (eds) Mauna Loa revealed: structure, composition, history, and hazards. Am Geophys Union Geophys Monogr 92:219–239

Ghiorso MS, Sack RO (1995) Chemical mass transfer in magmatic processes. IV. A revised and internally consistent thermodynamic model for the interpolation and extrapolation of liquid-solid equilibria in magmatic systems at elevated temperatures and pressures. Contrib Mineral Petrol 119:197–212

Gramlich JW, Lewis VA, Naughton JJ (1971) Potassium-argon dating of Holocene basalts of the Honolulu volcanic series. Geol Soc Am Bull 82:1399–1404

Guillou H, Sinton J, Laj C, Kissel C, Szeremeta N (2000) New K-Ar ages of shield lavas from Waianae Volcano, Oahu, Hawaiian Archipelago. J Volcanol Geotherm Res 96:229–242

Haggerty S, Baker I (1967) The alteration of olivine in basaltic and associated lavas. Part I. High temperature alteration. Contrib Mineral Petrol 16:233–257

Hauri EH (1996) Major-element variability in the Hawaiian mantle plume. Nature 382:415–419

Hauri EH (2002) SIMS analysis of volatiles in silicate glasses. 2. Isotopes and abundances in Hawaiian melt inclusions. Chem Geol 183:115–141

Hauri EH, Kurz MD (1997) Melt migration and mantle chromatography. 2. A time-series Os isotope study of Mauna Loa Volcano, Hawaii. Earth Planet Sci Lett 153:21–36

Hauri EH, Lassiter JC, DePaolo DJ (1996) Osmium isotope systematics of drilled lavas from Mauna Loa, Hawaii. J Geophys Res 101:11,793–11,806

Herrero-Bervera E, CaTapia E, Walker GPL, Guerrero-GarcC (2002) The Nuuanu and Wailau giant landslides: insights from paleomagnetic and anisotropy of magnetic susceptibility (AMS) studies. Phys Earth Planet Interiors 129:83–98

Hofmann AW, White WM (1982) Mantle plumes from ancient oceanic crust. Earth Planet Sci Lett 57:421–436

Jackson MC, Frey FA, Garcia MO, Wilmoth RA (1999) Geology and geochemistry of basaltic lava flows and dikes from the Trans-Koolau tunnel, Oahu, Hawaii. Bull Volcanol 60:381–401

Jakobsson SP (1972) On the consolidation and palagonitization of the tephra of the Surtsey volcanic island, Iceland. Surtsey Res Prog Rep 6:121–128

Jarosewich E, Nelen JA, Norberg JA (1979) Electron microprobe reference samples for mineral analyses. In: Fudali RF (ed) Mineral sciences investigations; 1976–1977. Smithsonian Contrib Earth Sci 22:68–69

Klein FW, Koyanagi RY, Nakata JS, Tanigawa WR (1987) The seismicity of Kīlauea's magma system. In: Decker RW, Wright TL, Stauffer PH (eds) Volcanism in Hawaii. USGS Prof Pap 1350:1019–1185

Kurz MD, Kenna TC, Kammer D, Rhodes JM, Garcia MO (1995) Isotopic evolution of Mauna Loa volcano: A view from the submarine southwest rift. Am Geophys Union Mono 92:289–306

Laj C, Szeremeta N, Kissel C, Guillou H (2000) Geomagnetic paleointensities at Hawaii between 3.9 and 2.1 Ma: preliminary results. Earth Planet Sci Lett 179:191–204

Lanphere MA, Dalrymple GB (1980) Age and strontium isotopic composition of the Honolulu volcanic series, Oahu, Hawaii. In: Irving AJ, Dungan MA (eds) The Jackson volume. Am J Sci 280 A(2):736–751

Lassiter JC, Hauri EH (1998) Osmium-isotope variations in Hawaiian lavas; evidence for recycled oceanic lithosphere in the Hawaiian Plume. Earth Planet Sci Lett 164:483–496

Lipman PW (1995) Declining growth of Mauna Loa during the last 100,000 Years: rates of lava accumulation vs. gravitational subsidence. In: Rhodes JM, Lockwood JP (eds) Mauna Loa revealed: structure, composition, history, and hazards. Am Geophys Union Geophys Monogr 92:45–80

Lipman PW, Rhodes JM, Dalrymple GB (1990) The Ninole basalt; implications for the structural evolution of Mauna Loa Volcano, Hawaii. Bull Volcanol 53:1–19

McDougall I (1964) Potassium-argon ages from lavas of the Hawaiian Islands. Geol Soc Am Bull 75:107–128

McDougall I, Brown FH, Cerling TE, Hillhouse JW (1992) A reappraisal of the geomagnetic polarity time scale to 4 Ma using data from the Turkana Basin, East Africa. Geophys Res Lett 19:2349–2352

Moore JG (1987) Subsidence of the Hawaiian Ridge. In: Decker RW, Wright TL, Stauffer PH (eds) Volcanism in Hawaii. USGS Prof Pap 1350:85–100

Moore JG, Clague DA, Holcomb RT, Lipman PW, Normark WR, Torresan ME (1989) Prodigious submarine landslides on the Hawaiian Ridge. J Geophys Res 94:17,465–17,484

Moore JG, Normark WR, Holcomb RT (1994) Giant Hawaiian underwater landslides. Science 264:46–47

Mukhopadhyay S, Lassiter JC, Farley KA, Bogue SW (2003) Geochemistry of Kauai shield-stage lavas: Implications for the chemical evolution of the Hawaiian plume. Geochem Geophys Geosyst 2003-01-24

Multhaup RA (1990) Subsurface mapping of basalts based on petrographic characterization of cuttings from borehole drilling on Oahu, Hawaii. MSc, University of Hawaii

Norman MD, Garcia MO (1999) Primitive magmas and source characteristics of the Hawaiian Plume; petrology and geochemistry of shield picrites. Earth Planet Sci Lett 168:27–44

Norman MD, Garcia MO, Kamenetsky VS, Nielsen RL (2002) Olivine-hosted melt inclusions in Hawaiian picrites: equilibration, melting, and plume source characteristics. Chem Geol 183:143–168

Norrish K, Hutton JT (1969) An accurate x-ray spectrographic method for the analysis of a wide range of geological samples. Geochim Cosmochim Acta 33:431–453

Pertermann M, Hirschmann M (2003) Anhydrous partial melting experiments on MORB-like eclogite: phase relations, phase compositions and mineral/melt partitioning of major elements at 2–3 GPa. J Petrol (in press)

Presley TK, Sinton JM, Pringle M (1997) Postshield volcanism and catastrophic mass wasting of the Waianae Volcano, Oahu, Hawaii. Bull Volcanol 58:597–616

Putirka K (1999) Melting depths and mantle heterogeneity beneath Hawaii and the East Pacific Rise; constraints from Na/Ti and rare earth element ratios. J Geophys Res 104:2,817–2,829

Quane SL, Garcia MO, Guillou H, Hulsebosch TP (2000) Magmatic history of the east rift zone of Kīlauea Volcano, Hawaii based on drill core from SOH 1. J Volcanol Geotherm Res 102:319–338

Rhodes JM (1996) Geochemical stratigraphy of lava flows sampled by the Hawaii Scientific Drilling Project. J Geophys Res 101:11,729–11,746

Roden MF, Frey FA, Clague DA (1984) Geochemistry of tholeiitic and alkalic lavas from the Koolau Range, Oahu, Hawaii; implications for Hawaiian volcanism. Earth Planet Sci Lett 69:141–158

Roden MF, Trull T, Hart SR, Frey FA (1994) New He, Nd, Pb, and Sr isotopic constraints on the constitution of the Hawaiian plume; results from Koolau Volcano, Oahu, Hawaii, USA. Geochim Cosmochim Acta 58:1431–1440

Satake K, Smith JR, Shinozaki K (2002) Volume estimate and tsunami modeling for the Nuuanu and Wailau landslides. In: Takahashi E, Lipman PW, Garcia MO, Naka J, Aramaki S (eds) Hawaiian volcanoes, deep underwater perspectives. Am Geophys Union Geophys Monogr 128:333–346

Seaman C, Garcia MG, Stolper EM (1999) Hawaii Scientific Drilling Project, California Institute of Technology, Pasadena, 1:3–7

Sharp W, Turrin B, Renne P, Lanphere M (1996), The $^{40}Ar/^{39}Ar$ and K/Ar dating of lavas from the Hilo 1-km core hold, Hawaiian Scientific Drilling Project. J Geophys Res 101:11,604–11,616

Shinozaki ZR, Ren Z, Takahashi E (2002) Geochemical and petrological characteristics of Nuuanu and Wailau landslide blocks. In: Takahashi E, Lipman PW, Garcia MO, Naka J, Aramaki S (eds) Hawaiian volcanoes, deep underwater perspectives. Am Geophys Union Geophys Monogr 128:297–310

Sinton CW, Christie DM, Duncan RA (1996) Geochronology of Galapagos seamounts. J Geophys Res 101:13,689–13,700

Sobolev AV, Hofmann AW, Nikogosian IK (2000) Recycled oceanic crust observed in 'ghost plagioclase' within the source of Mauna Loa lavas. Nature 404:986–989

Spell TL, Harrison TM (1993) $^{40}Ar/^{39}Ar$ geochronology of post-Valles Caldera rhyolites, Jemez volcanic field, New Mexico. J Geophys Res 98:8031–8051

Spell TL, McDougall I (2003) Characterization and calibration of $^{40}Ar/^{39}Ar$ dating standards. Chem Geol 198:189–211

Stearns HT (1939) Geologic map and guide of the Island of Oahu, Hawaii. Hawaii Div Hydrogr Bull 2

Steiger RH, Jaeger E (1977) Subcommission on geochronology: convention on the use of decay constants in geo and cosmochronology. Earth Planet Sci Lett 36:359–362

Stille P, Unruh DM, Tatsumoto M (1983) Pb, Sr, Nd and Hf isotopic evidence of multiple sources for Oahu, Hawaii basalts. Nature 304:25–29

Sun S, McDonough W (1989) Chemical and isotopic systematics of oceanic basalts: implications for mantle composition and processes. In: Magmatism in the ocean basins, Blackwell Scientific; Geological Society Special Publication 42:313–345

Takahashi E (1986) Melting study of a dry peridotite KLB-1 up to 14 GPa: implications on the origin of peridotitic upper mantle. J Geophys Res 91:9367–9382

Takahashi E, Nakajima K (2002) Melting process in the Hawaiian plume: an experimental study. In: Takahashi E, Lipman PW, Garcia MO, Naka J, Aramaki S (eds) Hawaiian volcanoes, deep underwater perspectives. Am Geophys Union Geophys Monogr 128:403–418

Tanaka R, Nakamura E, Takahashi E (2002) Geochemical evolution of Koolau volcano, Hawaii. In: Takahashi E, Lipman PW, Garcia MO, Naka J, Aramaki S (eds) Hawaiian volcanoes, deep underwater perspectives. Am Geophys Union Geophys Monogr 128:311–332

Wentworth CK (1951) Geology and ground-water resources of the Honolulu-Pearl Harbor area, Oahu, Hawaii. Honolulu, Hawaii Board Water Supply

Wentworth CK, Winchell H (1947) Koolau basalt series, Oahu, Hawaii. Geol Soc Am Bull 58:49–77

Winchell H (1947) Honolulu series, Oahu, Hawaii. Geol Soc Am Bull 58:1–48

Wright TL, Fiske RS (1971) Origin of the differentiated and hybrid lavas of Kīlauea volcano, Hawaii. J Petrol 12:1–65

Yaxley GM, Green DH (1998) Reactions between eclogite and peridotite: mantle refertilisation by subduction of oceanic crust. Schweiz Mineral Petrogr Mitt 78:243–255